

ItDPDM: Information-Theoretic Discrete Poisson Diffusion Model

Sagnik Bhattacharya^{1*} Abhiram R. Gorle^{1*} Ahmed Mohsin¹ Ahsan Bilal² Connor Ding¹
Amit Kumar Singh Yadav³ Tsachy Weissman¹

Abstract

Existing methods for generative modeling of discrete data, such as symbolic music tokens, face two primary challenges: (1) they either embed discrete inputs into continuous state-spaces or (2) rely on variational losses that only approximate the true negative log-likelihood. Previous efforts have individually targeted these limitations. While information-theoretic Gaussian diffusion models alleviate the suboptimality of variational losses, they still perform modeling in continuous domains. In this work, we introduce the Information-Theoretic Discrete Poisson Diffusion Model (ItDPDM), which simultaneously addresses both limitations by directly operating in a discrete state-space via a Poisson diffusion process inspired by photon arrival processes in camera sensors. We introduce a novel Poisson Reconstruction Loss (PRL) and derive an exact relationship between PRL and the true negative log-likelihood, thereby eliminating the need for approximate evidence lower bounds. Experiments conducted on the Lakh MIDI symbolic music dataset and the CIFAR-10 image benchmark demonstrate that ItDPDM delivers significant improvements, reducing test NLL by up to 80% compared to prior baselines, while also achieving faster convergence.

1. Introduction and Background

Denoising diffusion models have revolutionized generative modeling, surpassing GANs in image synthesis (Dhariwal & Nichol, 2021) and autoregressive models in density estimation (Kingma et al., 2021). Their adaptability has driven significant industrial applications, such as generating re-

alistic and diverse images from open-ended text prompts (Ramesh et al., 2022; Saharia et al., 2022b; Rombach et al., 2022), audio synthesis (Kong et al., 2021), and medical imaging tasks (Mulyukov et al., 2022). Diffusion models have also been effectively extended to multimodal domains, including text-to-image generation (Saharia et al., 2022a; Ramesh et al., 2022), video synthesis (Ho et al., 2022), cross-modal alignment tasks (Avrahami et al., 2022), and molecular modeling (Jing et al., 2022; Trippe et al., 2022).

Limitations of Existing Works: Diffusion models can be classified based on the intermediate timesteps being discrete (DT) or continuous (CT); and state-space being discrete (DS) or continuous (CS), leading to 4 categories: DTDS, DTCS, CTDS, and CTCS as shown in Figure 1. DTCS models such as variational diffusion models (VDMs) (Kingma et al., 2021) and CTCS information-theoretic Gaussian diffusion (Kong et al., 2023) are predominantly employed for continuous state modeling and thus excel in continuous domains (Ho et al., 2020; Kingma et al., 2021). However, these continuous-state approaches are suboptimal for inherently discrete data such as image pixels or symbolic music tokens. As shown in Figure 1, to handle discrete data, these frameworks typically embed discrete inputs into continuous spaces using pre-processing techniques like z-scoring (Chen et al., 2021), tail normalization (Hooeboom et al., 2021), or uniform dequantization (Kong et al., 2023). Nevertheless, such methods fail to bridge the discretization gap (e.g., $\frac{1}{127.5}$ for normalized image pixel values), forcing models to learn suboptimal probability density functions (pdf) (Kong et al., 2023), rather than probability mass functions (pmf). As noted in (Kong et al., 2023), the necessity to discretize outputs during post-processing leads to a train-test mismatch, further degrading the generative quality (Austin et al., 2021; Nguyen et al., 2023). Recent research attempts to directly model in the discrete domain, addressing these limitations by avoiding embedding into continuous spaces altogether.

Discrete-time discrete-state (DTDS) models (Austin et al., 2021; Hooeboom et al., 2021; Plasser et al., 2023) perform modeling in discrete domain and have better performance than variational Gaussian-based model. However, these methods disregard ordinal structure in integer-valued data during modeling and need post-processing. Another recent approach “Learning-to-Jump” (LTJ) (Chen & Zhou,

^{*}Equal contribution ¹Department of Electrical Engineering, Stanford University, Stanford, CA, USA ²Department of Computer Science, Oklahoma University, Norman, OK, USA ³School of Electrical and Computer Engineering, Purdue University, West Lafayette, Indiana, USA. Correspondence to: Sagnik Bhattacharya <sagnikb@stanford.edu>.

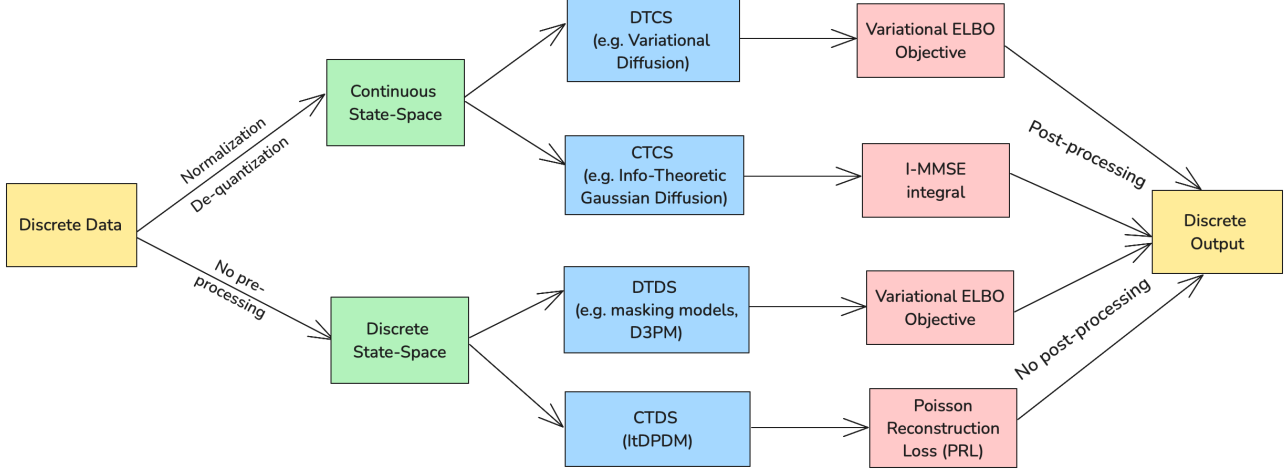


Figure 1. Classification of diffusion models. Discrete data can be modeled via continuous or discrete state-spaces.

2023) method performs discrete-domain modeling using a binomial thinning chain with approximate variational loss function. LTJ surpasses previous DTDS and variational Gaussian diffusion models but faces two critical limitations: (1) its variational evidence lower bound (ELBO) loss-based training involves a per-step relative-entropy loss without an exact closed-form likelihood, resulting in approximate likelihood estimation, and (2) discrete decoding requires exactly T Markov steps, limiting flexibility and necessitating careful scheduling.

Main Contributions. To address these limitations, we propose a novel **Discrete Poisson Diffusion Model (ItDPDM)**. As shown in Figure 1, contrary to Gaussian diffusion, ItDPDM directly models discrete non-negative data using Poisson noise, avoiding the need for soft discretization or dequantization.

We also demonstrate the efficacy of the proposed model on inherently discrete datasets such as 2D CIFAR image data and 1D symbolic music benchmarks. Our main contributions are as follows:

- A novel information-theoretic **Poisson Diffusion Model (ItDPDM)** that models data generation as a Poisson arrival process. We introduce a novel information-theoretic *poisson reconstruction loss* (PRL) to address the suboptimality of variational objectives in (Chen & Zhou, 2023; Kingma et al., 2021). This objective leverages the information-theoretic link between negative log-likelihood (NLL) and mean-likelihood error poisson reconstruction loss (PRL) for improved discrete density estimation. Using this improved PRL objective, we also derive exact relationships between the data probability distribution and the denoiser under the proposed loss function.
- We formulate an information-theoretic I-MPRL frame-

work for the Poisson channel, deriving an exact relationship between negative log-likelihood and our proposed minimum PRL (mprl) estimator:

$$-\log P(x) = \int_0^\infty \text{mprl}(x, \gamma) d\gamma + \text{constant}, \quad (1)$$

This exact expression enables direct optimization of discrete probability mass functions without any probability density approximation.

- While variational diffusion models (Kingma et al., 2021) resort to approximate ELBO losses, we derive and implement an exact negative log-likelihood (NLL) formulation of the data distribution in terms of a function of the MPRL estimator. Minimizing this improved loss function leads to lower NLL values than variational methods.
- For ease of implementation, we derive tight upper bounds on the exact NLL formulation, using tail integration bounds and importance sampling-aided PRL

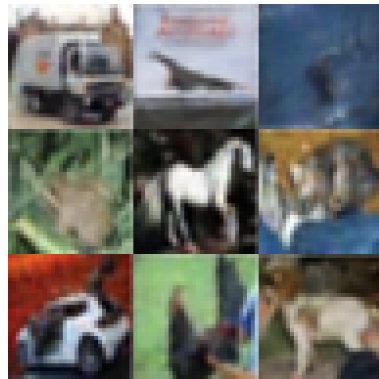


Figure 2. Unconditional image generation (ItDPDM) on CIFAR10.

summations over varying signal-to-noise ratio (SNR) values. On training ItDPDM with this loss function, it leads to 1) lower NLL values, 2) faster convergence on discrete positive data, e.g. CIFAR images and Lakh MIDI symbolic music datasets, compared to variational and information-theoretic Gaussian diffusion methods. The efficacy of the PRL objective is also demonstrated using a cross-training paradigm.

This work presents a proof-of-concept for discrete information-theoretic Poisson diffusion models, demonstrating initial advantages over Gaussian approaches in denoising and generating discrete positive-valued data, without claiming state-of-the-art status.

2. Information-Theoretic Diffusion

We briefly go over the Information-Theoretic Gaussian Diffusion (ITDiff) framework from (Kong et al., 2023), which helps us draw parallels to the proposed Poisson Diffusion in Section 4. The Gaussian noise channel is defined as

$$z_\gamma = \sqrt{\gamma}x + \epsilon, \quad \epsilon \sim \mathcal{N}(0, I), \quad (2)$$

with signal-to-noise ratio (SNR) parameter γ and data distribution $p(x)$. A key issue in this framework is the exploding variance at high SNR levels.

Relating Minimum Mean Square Error (MMSE) to Mutual Information

The ‘‘I-MMSE’’ relation (Guo et al., 2005) links mutual information with the MMSE (minimum mean square error) estimator:

$$\frac{d}{d\gamma} I(x; z_\gamma) = \frac{1}{2} \text{mmse}(\gamma), \quad (3)$$

where the MMSE is defined as:

$$\text{mmse}(\gamma) = \min_{\hat{x}(z_\gamma, \gamma)} \mathbb{E}_{p(z_\gamma, x)} [\|x - \hat{x}(z_\gamma, \gamma)\|_2^2] \quad (4)$$

A pointwise generalization of Eq. (3) extends to KL divergence:

$$\frac{d}{d\gamma} D_{KL}(p(z_\gamma|x) \| p(z_\gamma)) = \frac{1}{2} \text{mmse}(x, \gamma). \quad (5)$$

Variational Formulation and Log-Density Estimation

This relation leads to an exact variational form of the VLB for diffusion models (Kingma et al., 2021):

$$\begin{aligned} -\log p(x) &= D_{KL}[p(z_{\gamma_1}|x) \| p(z_{\gamma_1})] \\ &\quad + \mathbb{E}_{p(z_{\gamma_0}|x)} [-\log p(x|z_{\gamma_0})] \\ &\quad + \frac{1}{2} \int_{\gamma_0}^{\gamma_1} \text{mmse}(x, \gamma) d\gamma. \end{aligned} \quad (6)$$

Recent work highlights inefficiencies in this decomposition when applied to discrete data reconstruction. (Kong et al., 2023) derives an exact non-variational form of the data log-density:

$$\begin{aligned} -\log p(x) &= \frac{d}{2} \log(2\pi e) \\ &\quad - \frac{1}{2} \int_0^\infty \left(\frac{d}{1+\gamma} - \text{mmse}(x, \gamma) \right) d\gamma. \end{aligned} \quad (7)$$

This expression shows that the density estimate depends only on the optimal denoising MSE (mean square error) loss. Its pointwise generalization provides a probability estimator for discrete distributions:

$$-\log P(x) = \frac{1}{2} \int_0^\infty \text{mmse}(x, \gamma) d\gamma. \quad (8)$$

3. Poisson Diffusion Formulation

3.1. Poisson Noise Channel

We now introduce the canonical Poisson noise channel where, given a non-negative input $x \geq 0$, the output on passing x through the Poisson channel with SNR γ is given by z_γ . The probability mass function (PMF) of z_γ , P is given as: (from here on, we use \mathcal{P} to denote the Poisson distribution)

$$P(z_\gamma|x) = \mathcal{P}(\gamma x) = \frac{(\gamma x)^{z_\gamma} e^{-(\gamma x)}}{z_\gamma!}, \quad z_\gamma = 0, 1, 2, \dots, \quad (9)$$

Our work is inspired by a channel which is commonly seen in direct-detection optical communication systems (Verdú, 2004; Bar-David, 1969) where incident radiation is intercepted using photon-sensitive devices to result in a Poisson process, the rate of which is the intensity of radiation added to ‘‘dark current’’ (arising as a result of noise in the device (Shamai & Wyner, 1990))

3.2. Diffusion using Poisson channel

We propose an information-theoretic Poisson diffusion process. Let x be the source signal with some unknown distribution $p(x)$, and let the diffusion step at (SNR) γ produce z_γ , where:

$$z_\gamma \sim \mathcal{P}(\gamma x) \quad (10)$$

As evident from the above Eq. (10), this leads to discrete positive integer outputs at every SNR γ . To model discrete data in any other domain (like discrete non-integer values in $[-1, 1]$ range), the outputs from Eq. (10) can be normalized to yield values in the appropriate range. A crucial point to note is that, unlike the Gaussian noise scenario, where the noisy signal can be separated into the clean signal and the noise, the Poisson noise is non-additive and does not have the property of being source-separable. Figure 3 illustrates a comparison of Gaussian and Poisson diffusion processes along with their respective denoising trajectories.

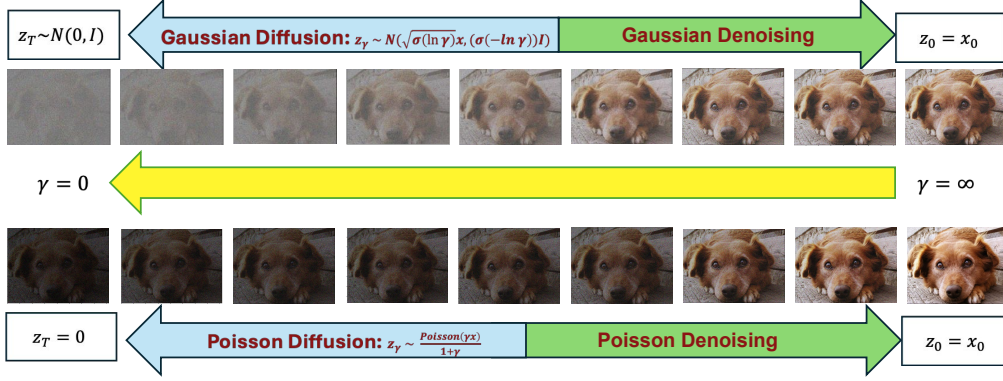


Figure 3. Visual comparison of Gaussian and Poisson diffusion processes and their respective denoising trajectories.

3.3. Novel Poisson Loss Function

The function $l_0(x) = x \log x - x + 1$, $x > 0$ (where \log denotes the natural logarithm throughout) is the convex conjugate of the Poisson distribution’s log moment generating function (proof in Appendix A.1) and often arises naturally in the analysis of Poisson and continuous-time jump Markov processes in a variety of situations (Dupuis & Ellis, 1995) and notably, for the estimation of the mutual information in the Poisson channel (Liptser & Shiryaev, 2001).

Building on this foundation, we define the **poisson reconstruction loss** $l(x, \hat{x})$ as:

$$l(x, \hat{x}) = \hat{x} l_0(x/\hat{x}) = x \log \left(\frac{x}{\hat{x}} \right) - x + \hat{x}, \quad (11)$$

We also define the minimum poisson reconstruction loss (MPRL) in a form analogous to the MMSE, as:

$$\text{mprl}(\gamma) \equiv \min_{\hat{x}(z_\gamma, \gamma)} E_{P(z_\gamma, x)} [l(x, \hat{x}(z_\gamma, \gamma))], \quad (12)$$

where we refer to $\hat{x}(z_\gamma, \gamma)$ as the denoiser. The optimal denoiser function \hat{x}^* corresponds to the conditional expectation of x given z_γ , $E[X|Z_\gamma]$ and can be derived using variational calculus or from the fact that the Poisson loss function we defined belongs to the class of Bregman divergences (Banerjee et al., 2005): (proof in Appendix A.1)

$$\hat{x}^*(z_\gamma, \gamma) \equiv \arg \min \text{mprl}(\gamma) = E_{x \sim P(x|z_\gamma)}[x] \quad (13)$$

The analytical solution is typically intractable because it requires sampling from the posterior distribution of the Poisson noise channel. Next, we also outline key properties (Atar & Weissman, 2010) of this loss function indicating it is a natural choice for measuring the reconstruction quality of non-negative objects, similar to the squared error loss in the Gaussian setting.

Lemma 3.1 (Poisson Reconstruction Loss). *The loss function $l(x, \hat{x})$ satisfies the following properties:*

1. **Non-negativity:** $l(x, \hat{x}) \geq 0$, with equality if and only if $x = \hat{x}$.
2. **Convexity:** $l(x, \hat{x})$ is convex in \hat{x} for each fixed x , and in x for each fixed \hat{x} .
3. **Scaling:** For any $\alpha > 0$, $l(\alpha x, \alpha \hat{x}) = \alpha l(x, \hat{x})$.
4. **Unboundedness for underestimation:** For any $x > 0$, $\lim_{\hat{x} \rightarrow 0^+} l(x, \hat{x}) = \infty$.
5. **Optimality of Conditional Expectation:** For any non-negative random variable X with $E[X \log^+ X] < \infty$, the conditional expectation $E[X|Y]$ uniquely minimizes the expected loss $E[l(X, \hat{x})]$

Convexity makes the loss amenable to gradient-based methods. Property 4 strongly penalizes underestimation, making $l(x, \hat{x})$ particularly suitable for non-negative data. Notably, common loss functions such as absolute or squared error do not possess this property. The last property mirrors the optimality of conditional expectation under MSE and underscores the suitability of $l(x, \hat{x})$ for estimation in the Poisson noise channel. Our novel Poisson loss function is also illustrated below in Figure 4.

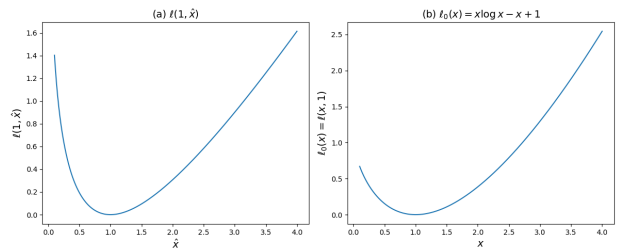


Figure 4. The loss function l

As per Lemma 3.1, the conditional expectation $E[X|Y]$ uniquely minimizes the expected “mprl” loss function. We now look into this conditional expectation.

Conditional Expectation for Poisson Channel We define the angle bracket operator for X as its conditional expectation given Z_γ : $\langle X \rangle = E[X|Z_\gamma]$. Notably, for the Poisson channel, $\langle \cdot \rangle$ is nonlinear, since $\langle \alpha X + \lambda \rangle \neq \alpha \langle X \rangle + \lambda$ for $\alpha \neq 1$ and $\lambda > 0$. This nonlinearity contrasts with the Gaussian case, where the conditional expectation $\langle X \rangle$ is linear (Bishop, 2006) – a widely used paradigm in estimation theory. This highlights the increased complexity of Poisson-based transforms, making Poisson diffusion-based denoising significantly more challenging than the Gaussian case. Nevertheless, the optimal estimator in the Poisson channel is also linear under the following conditions. Let $\langle X \rangle_z$ denote $\langle X \rangle$ evaluated at $Z_\gamma = z$, then:

Lemma 3.2 (Linearity in Poisson Channel). *Let $Z_\gamma = \mathcal{P}(\gamma X)$. Then, $\langle X \rangle_z = az + b$, if and only if $X \sim \text{Gam}(\frac{1-\gamma a}{a}, \frac{b}{a})$ for any $0 < a < \frac{1}{\gamma}$ and $b > 0$.*

While the proof for a general Poisson channel is involved, it becomes simpler here since the Gamma distribution is a conjugate prior distribution of the Poisson distribution (Diaconis & Ylvisaker, 1979). Using this fact, the conditional variance also turns out to be linear for a Gamma prior – proof in Appendix A.1 (in contrast, it is independent of the observation in the Gaussian case). Now, we revisit the squared error (SE) loss function before stating our next property. Consider $l_{\text{SE}}(x, \hat{x}) = (x - \hat{x})^2$, which satisfies, for any random variable X of finite variance,

$$E[l_{\text{SE}}(X, \hat{x})] = E[l_{\text{SE}}(X, E[X])] + l_{\text{SE}}(E[X], \hat{x}). \quad (14)$$

We show that our Poisson loss function has a similar property below:

Lemma 3.3. *For any non-negative random variable X with $E[X \log^+ X] < \infty$, and any $\hat{x} \in [0, \infty)$,*

$$E[l(X, \hat{x})] = E[l(X, E[X])] + l(E[X], \hat{x}).$$

Proof. When $X = 0$ almost surely, $E[X] = 0$, and the identity holds by convention. Else, $E[X] > 0$, and we have:

$$\begin{aligned} E[l(X, \hat{x})] &= E\left[X \log\left(\frac{X}{\hat{x}}\right) - X + \hat{x}\right] \\ &= E[X \log X] - E[X \log \hat{x}] - E[X] + \hat{x} \\ &= E[X \log X - X \log E[X] - X + E[X]] \\ &\quad + l(E[X], \hat{x}) \\ &= E[l(X, E[X])] + l(E[X], \hat{x}). \end{aligned}$$

A result that immediately follows from Lemma (3.3), when combined with the non-negativity property in Lemma 3.1, is that $E[X]$ uniquely minimizes $E[l(X, \hat{x})]$ over all \hat{x} :

$$\min_{\hat{x}} E[l(X, \hat{x})] = E[l(X, E[X])] \quad (15)$$

$$= E[X \log X] - E[X] \log E[X]. \quad (16)$$

Consequently, the above equation also elegantly shows that the conditional expectation is the optimal estimator even for

the Poisson loss function. The conditional expectation over a Poisson noise channel also has other unique properties, some of which are stated below. An interesting property of the optimal estimator in a Poisson noise channel is that it depends solely on the marginal distribution of Z_γ . This result is originally known as the *Turing-Good-Robbins* formula (Good, 1953; Robbins, 1956). This formula draws parallels with the Discrete Universal Denoiser (DUDE) (Weissman et al., 2005), which estimates original discrete symbols from noisy observations by leveraging local empirical probabilities.

Lemma 3.4. *Let $Z_\gamma = \mathcal{P}(\gamma X)$. Then, for every $\gamma > 0$,*

$$\langle X \rangle_z = \frac{1}{\gamma} \frac{(z+1)P_{Z_\gamma}(z+1)}{P_{Z_\gamma}(z)}, \quad z = 0, 1, \dots$$

The next property is useful in showing that the conditional expectation in this case is unique for every input distribution.

Lemma 3.5. *Let $Z_\gamma = \mathcal{P}(\gamma X)$. Then, for every positive integer k and every non-negative integer z ,*

$$E[(\gamma X)^k | Z_\gamma = z] = \prod_{i=0}^{k-1} E[\gamma X | Z_\gamma = z + i].$$

Our novel poisson reconstruction loss $l(x, \hat{x})$ therefore provides a natural objective for diffusion models operating on non-negative discrete data. Unlike the squared error loss, which assumes continuous outputs and requires post-hoc quantization, $l(x, \hat{x})$ directly models discrete probability mass functions, avoiding quantization artifacts. Using the properties above, we formulate a pointwise denoising relation for Poisson channel as follows:

$$\frac{d}{d\gamma} D_{KL}[P(z_\gamma|x) \| P(z_\gamma)] = \text{mprl}(x, \gamma), \quad (17)$$

where $p(z_\gamma) = \int p(z_\gamma|x)p(x)dx$ is the marginal distribution, and **pointwise MPRL** is defined as:

$$\text{mprl}(x, \gamma) \equiv E_{P(z_\gamma|x)}[l(x, \hat{x}(z_\gamma, \gamma))] \quad (18)$$

The **pointwise MPRL** is the MPRL evaluated at a single point x , and the expectation of over $p(x)$ trivially recovers the MPRL defined earlier. Taking the expectation with respect to x of both sides of Eq. (17) recovers the generalized I-MPRL relationship in Eq. (19). When a mismatched estimator (Atar & Weissman, 2010) is used, the integral of excess mean loss over the parameter range equals the relative entropy between true and mismatched distributions, which can be directly established using Eq. 17.

I-MPRL relation. As mentioned earlier, (Kong et al., 2023) makes effective use of the seminal result from (Guo et al., 2005), that connects the derivative of mutual information between the input and output of the channel to the minimum mean-squared error (MMSE) in the Gaussian noise channel. We establish and make use of the I-MPRL relation for the Poisson noise channel which can be stated as:

$$\frac{d}{d\gamma} I(x; z_\gamma) = \text{mprl}(\gamma), \quad (19)$$

Interestingly, a similar elegant relation also exists for the derivative with respect to the “dark current” in a general Poisson channel. Using the “incremental channel” device introduced in (Guo et al., 2005), we provide a detailed proof of both these results in Appendix A.3. For our Poisson channel, we also have:

Lemma 3.6. *Let $Z_\gamma = \mathcal{P}(\gamma X)$. Then, for every $\gamma > 0$ and $y = 0, 1, \dots$,*

$$\frac{d}{d\gamma} P_{Z_\gamma|X}(y|x) = x (P_{Z_\gamma|X}(y-1|x) - P_{Z_\gamma|X}(y|x)),$$

and

$$\gamma \frac{d}{d\gamma} P_{Z_\gamma}(y) = y P_{Z_\gamma}(y) - (y+1) P_{Z_\gamma}(y+1),$$

where $P_{Z_\gamma|X}(-1|x) = P_{Z_\gamma}(-1) = 0$.

This approach allows us to derive exact relationships between the Poisson loss function we proposed and the mutual information, thereby enabling us to establish upper bounds on the log-likelihood and reinforce the information-theoretic foundations of Poisson Diffusion. Detailed proofs of Lemmas (3.1), (3.2), (3.4), (3.5) and (3.6) are presented in Appendix A.2.

4. ItDPDM: Information-Theoretic Poisson Diffusion

4.1. Thermodynamic Integration for Variational Bound

Using our pointwise denoising relation, we derive a log-likelihood expression akin to the variational bound. Unlike traditional methods requiring costly sampling, diffusion models exploit the noise channel’s properties for efficient sampling at any noise level (Brekelmans et al., 2020). This enables stable training via the convexity of the Poisson loss function. Now, let $P(z_\gamma|x)$ denote a Poisson noise channel with rate γx . Thermodynamic integration techniques outlined in (Ogata, 1989; Gelman & Meng, 1998) yield:

$$\int_{\gamma_0}^{\gamma_1} \frac{d}{d\gamma} D_{KL}[P(z_\gamma|x) \parallel P(z_\gamma)] d\gamma = - \int_{\gamma_0}^{\gamma_1} \text{mprl}(x, \gamma) d\gamma, \quad (20)$$

where $\text{mprl}(x, \gamma) \equiv \mathbb{E}_{P(z_\gamma|x)} [l(x, \hat{x}^*(z_\gamma, \gamma))]$ is the pointwise MPRL for Poisson denoising. The exact log-likelihood is given by:

$$\begin{aligned} -\log P(x) &= \underbrace{D_{KL}[P(z_{\gamma_1}|x) \parallel P(z_{\gamma_1})]}_{\text{Prior loss}} \\ &+ \underbrace{E_{P(z_{\gamma_0}|x)}[-\log P(x|z_{\gamma_0})]}_{\text{Recon. loss}} - \underbrace{\int_{\gamma_0}^{\gamma_1} \text{mprl}(x, \gamma) d\gamma}_{\text{Diffusion loss}}. \end{aligned} \quad (21)$$

We also outline a possible extension of the proposed Continuous-Time Discrete-State Poisson Diffusion to a Continuous-Time Continuous-State equivalent of (Kong et al., 2023) in Appendix D.

4.2. Discrete Probability Estimator using MPRL

We now derive our novel discrete probability estimator in the case of a Poisson channel. Consider a discrete random variable $x \sim P(x)$ and $Z_\gamma \sim \mathcal{P}(\gamma x)$. Leveraging thermodynamic integration, we derive a novel discrete probability estimator below. Taking limits $\gamma_0 \rightarrow \infty$ and $\gamma_1 \rightarrow 0$, we have both prior and reconstruction loss going to zero:

$$D_{KL}[P(z_{\gamma_1}|x) \parallel P(z_{\gamma_1})] + E_{P(z_{\gamma_0}|x)}[-\log P(x|z_{\gamma_0})] = 0.$$

This finally gives us:

$$-\log P(x) = \int_0^\infty \text{mprl}(x, \gamma) d\gamma, \quad (22)$$

where $\text{mprl}(x, \gamma)$ denotes the minimum mean likelihood error for Poisson denoising at parameter γ . To obtain an expression resembling the variational bound, we take the expectation of both sides with respect to $x \sim P(x)$:

$$\begin{aligned} E[-\log P(x)] &= E \left[\int_0^\infty \text{mprl}(x, \gamma) d\gamma \right] \\ &= \int_0^\infty E[\text{mprl}(x, \gamma)] d\gamma = \int_0^\infty E[l(X, \hat{x}^*)] d\gamma \\ &= \int_0^\infty E[X \log X - E[X|Z_\gamma] \log E[X|Z_\gamma]] d\gamma \\ &= \int_0^\infty E \left[X \log \frac{X}{E[X|Z_\gamma]} \right] d\gamma. \end{aligned} \quad (23)$$

where $\hat{x}^*(X, \gamma) = E[X|Z_\gamma]$ is the optimal estimator.

Additionally, as shown in (Dytso & Vincent Poor, 2020), for a Poisson channel $Z_\gamma = \mathcal{P}(aX + \lambda)$, the sequence of conditional expectations $\{\mathbb{E}[X|Z_\gamma = z]\}_{z \geq 0}$ uniquely determines the input distribution P_X . This result complements our information-theoretic derivation, and provides further rigor for discrete-state noise models. We also outline an equivalent score matching function of the well-known Tweedie’s formula for Poisson denoising in Appendix C.1

5. Numerical Details

MPRL Upper Bound.

A key challenge is the inaccessibility of the posterior distribution. To address this, we analyze the estimation gap between the optimal conditional expectation and the suboptimal estimator $\hat{X}(Z_\gamma, \gamma)$ from the Poisson diffusion model. We express the expected loss in terms of the optimal estimator (using shorthand notation subsequently):

$$E[l(X, \hat{X}(X, \gamma))] = E \left[X \log \frac{X}{\hat{X}(X, \gamma)} - X + \hat{X}(X, \gamma) \right] \quad (24)$$

$$E \left[X \log \frac{X}{\hat{X}^*} \right] + E \left[X \log \frac{\hat{X}^*}{\hat{X}} - X + \hat{X} \right].$$

Using the law of iterated expectation gives:

$$E[l(X, \hat{X})] = \text{mprl}(\gamma) + E[l(\hat{X}^*, \hat{X})].$$

The second term above denotes the estimation gap, and rearranging the terms, we get:

$$E[-\log P(X)] = \int_0^\infty \left(E[l(X, \hat{X}^*)] - E[l(\hat{X}^*, \hat{X})] \right) d\gamma.$$

Using Jensen's inequality here (based on the properties mentioned in 3.1), we have:

$$\begin{aligned} -E[l(\hat{X}^*, \hat{X})] &\leq -E[\hat{X}^*] \log \frac{E[\hat{X}^*]}{\hat{X}} \\ &\quad - E[\hat{X}^*] + \hat{X} = -l(E[X], \hat{X}). \end{aligned} \quad (25)$$

Now, using the relation from 3.2 gives us:

$$\int_0^\infty \text{mprl}(\gamma) d\gamma \leq \int_0^\infty E[l(X, E[X])] d\gamma. \quad (26)$$

We obtain a more elegant bound in terms of the suboptimal denoiser by dropping the negative term, leading to:

$$E[-\log P(x)] = \int_0^\infty \text{mprl}(\gamma) d\gamma \leq \int_0^\infty E[l(X, \hat{x})] d\gamma. \quad (27)$$

Parametrization. To ensure stability across SNR levels, we reparameterize the Poisson observation $Z_\gamma \sim \mathcal{P}(\gamma X)$ to mitigate variance explosion. Instead of feeding Z_γ directly into the neural network, we define $\tilde{Z}_\gamma = Z_\gamma / (1 + \gamma)$, keeping it within $[0, X]$ with high probability. This transformation maintains interpretability: at high SNR, $E[\tilde{Z}_\gamma] \approx X$, while at low SNR ($\gamma \rightarrow 0$), it ends to zero, aligning with Poisson behavior. We input $(\tilde{Z}_\gamma, \gamma)$ into the network rather than (Z_γ, γ) . Using the log-SNR parameterization $\alpha = \log \gamma$, the formulation extends over the range (γ_0, γ_1) :

$$E[-\log P(x)] = \int_0^\infty \text{mprl}(\gamma) d\gamma \leq \int_{\alpha_0}^{\alpha_1} E[l(X, \hat{x})] d\alpha. \quad (28)$$

Numerical Integration. The next part involves computing the integral in an efficient manner. We first use importance sampling to rewrite the integral as an expectation over a distribution, $q(\gamma)$, allowing for unbiased Monte Carlo estimation. This leads to our final numerical approximation of the loss function $E_{p(x)}[-\log p(x)] \leq \mathcal{L}$, where

$$\mathcal{L} \equiv E_{q(\alpha)} \left[\frac{1}{q(\alpha)} E_{(x, z_\gamma)} [l(X, \hat{x})] \right].$$

We propose two paradigms for the numerical integration, the **Logistic** and **Uniform** Integration, respectively.

Logistic Integration. In Gaussian diffusion models, the log-SNR integral is approximated via importance sampling with a truncated logistic distribution. The integrand, shaped by a mixture of logistic CDFs influenced by data covariance eigenvalues λ_i , is captured by matching the empirical mean μ and variance s of $-\log \lambda_i$, with integration bounds $[\mu - 4s, \mu + 4s]$. Samples drawn via the logistic quantile function are weighted by $1/q(\alpha)$ to prioritize critical regions, reducing variance.

Uniform Integration. This simpler numerical method discretizes the log-SNR range $[\alpha_1, \alpha_2]$ into a uniform grid, applying trapezoidal or Riemann-sum integration without assuming an underlying distribution. While simple, efficiency depends on grid density for broad ranges, favoring ease over optimal sampling. The predefined range is $[-28, 37]$ with uniform sampling.

MPRL Tail Bounds. From equation 22, we derived the following negative log-likelihood (NLL) expression:

$$\mathbb{E}[-\log P(x)] = \int_0^\infty \text{mprl}(\gamma) d\gamma$$

Now, if our relevant range of integration (found empirically) is (γ_0, γ_1) , we can write this as:

$$\begin{aligned} &= \int_{\gamma_0}^{\gamma_1} \text{mprl}(\gamma) d\gamma + \left(\int_0^{\gamma_0} + \int_{\gamma_1}^\infty \right) \text{mprl}(\gamma) d\gamma \\ &\leq \int_{\gamma_0}^{\gamma_1} \mathbb{E}_{p(z_\gamma|x)} [l(x, \hat{x}^*(z_\gamma, \gamma))] d\gamma + f(\gamma_0, \gamma_1) \end{aligned}$$

We analytically derive upper bounds for the left and right tail integrals shown above, and denoted by $f(\gamma_0, \gamma_1)$ above in Appendix B, which are as follows: (we assume an $x \in \mathcal{X} \subset \mathbb{Z}^d$, with a domain that is discrete but numeric)

Left Tail: (an exponential prior on X achieves this)

$$\int_0^{\gamma_0} \text{mprl}(\gamma) d\gamma \leq \frac{\gamma_0}{2} \sum_{i=1}^d \frac{1}{\lambda_i} \quad (29)$$

Right Tail: (c_{ij} are Chernoff-type data-dependent parameters)

$$\int_{\gamma_1}^\infty \text{mprl}(\gamma) d\gamma \leq \sum_{i=1}^d \sum_{j=1}^{j_{\max}} \left[x_i \log \left(\frac{x_i}{x_i - j\Delta} \right) - j\Delta \right] \frac{e^{-c_{ij} \gamma_1}}{c_{ij}} \quad (30)$$

In Section 5, we have a practical upper bound using the suboptimal denoiser obtained from the Poisson diffusion model.

6. Experimental Results

6.1. Diffusion Details

We evaluate our Poisson Diffusion Model (ItDPDM) against Gaussian diffusion baselines on two discrete-datasets: CIFAR-10 image dataset and LAKH MIDI symbolic music dataset. Unlike (Kong et al., 2023), where pre-trained models are used and finetuned using an improved optimization objective, there are no analogous pre-trained Poisson diffusion models. This motivates the need to train from scratch in our case. For a fair comparison, all models are trained from scratch under identical architectures (U-Net (Ronneberger et al., 2015) for images, NCSN backbone (Song & Ermon, 2019) for music). We further also compare against pre-trained models like DDPM (Ho et al., 2020) and an Improved DDPM (IDDPM) (Nichol & Dhariwal, 2021) to contextualize performance.

Datasets: For the following experiments, we use the CIFAR and Lakh MIDI (LMD) datasets scaled appropriately as outlined in the next section. The ubiquitously used CIFAR-10 dataset consists of 60,000 (32×32) color images across 10 classes (Krizhevsky, 2009). The well-known LMD for symbolic music contains 648,574 samples, each with 256 notes represented by integers from 0 to 89, where ‘0’ denotes a rest, ‘1’ indicates a continuation of previous note, and 2–89 correspond to actual note pitches (Vogl et al., 2017). The preprocessing steps we use for symbolic music (LMD) are described in Appendix E.1.

Data and Model Normalization: We experimented with various schemes for data (Dn) before passing it through the noisy channel and for model inputs (Mn) post-noising. CIFAR-10 data is normalized to $[0, 1]$, $[1, 2]$, $[0, 255]$, $[-1, 1]$; Lakh MIDI to $[0, 1]$, $[1, 2]$, $[0, 90]$, $[-1, 1]$. Poisson channels cannot handle negatives and since zero inputs yield zeros, we shift inputs by $\epsilon = 10^{-6}$. For Gaussian noising, model normalization used $[0, 1]$ or $[-1, 1]$, while Poisson noising used only $[0, 1]$. The best results were achieved with $[-1, 1]$ (Gaussian) and $[1, 2]$ (Poisson) for Dn, and $[-1, 1]$ (Gaussian) and $[0, 1]$ (Poisson) for Mn. Among the integration paradigms used, logistic integrate yielded the best empirical results, and the `loc` and `scale` parameters obtained for the mid-integral range were (6, 3) for Gaussian noising and $(-1, 5)$ for Poisson noising. For numerical integration, the number of log SNR samples we used were $n = 1000$.

6.2. Denoiser Architecture

For CIFAR-10 images, we employ a U-Net architecture (Ronneberger et al., 2015) with residual blocks and self-attention layers. The encoder comprises four downsampling blocks (convolution \rightarrow GroupNorm \rightarrow SiLU) that reduce spatial resolution from 32×32 to 4×4 , followed by a

Table 1. Negative Log-Likelihood, $E[-\log P(x)]$ on CIFAR Test Data (bits per dimension):

*checkpoint models provided by (Kong et al., 2023) directly used

Noise + Loss Function	DDPM	IDDPM
ITDiff ((Kong et al., 2023))*	2.97	0.86
Gaussian + MSE	0.44	0.48
Gaussian + PRL (ours)	0.27	0.32
Poisson + MSE (ours)	0.23	0.22
ItDPDM: Poisson + PRL (ours)	0.18	0.17

bottleneck with self-attention at 8×8 resolution. The decoder mirrors the encoder via transposed convolutions and skip connections. For symbolic music synthesis on Lakh MIDI, we adapt an NCSN++ backbone (Song & Ermon, 2019) with a Transformer encoder (Vaswani et al., 2017). The architecture includes a 512-dimensional embedding layer, six transformer layers with multi-head attention (8 heads) and positional encodings, and time-dependent noise conditioning.

6.3. Performance Comparison: Negative Log Likelihood

Table 1 presents the average negative log likelihood (NLL) on test data (a subset of CIFAR) for our proposed and baseline models. We compare against two baselines: (1) **ITDiff** (Kong et al., 2023), a checkpoint of their finetuned Gaussian DDPM and IDDPM models based on available pretrained models, and (2) **Gaussian + MSE**, DDPM and IDDPM models trained from scratch using ITDiff’s information-theoretic Gaussian diffusion loss to ensure a fair comparison to our Poisson diffusion model, for which there exists no pretrained architectures. Our proposed **ItDPDM** (Poisson + PRL), with the PRL loss function, outperforms both baselines across DDPM and IDDPM architectures,

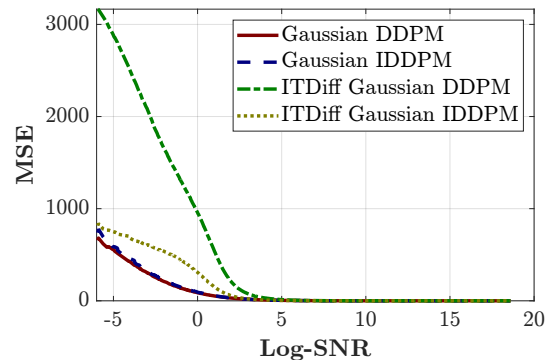


Figure 5. Test MSE versus logSNR values for Gaussian diffusion models trained from scratch, and checkpoint models taken from (Kong et al., 2023)

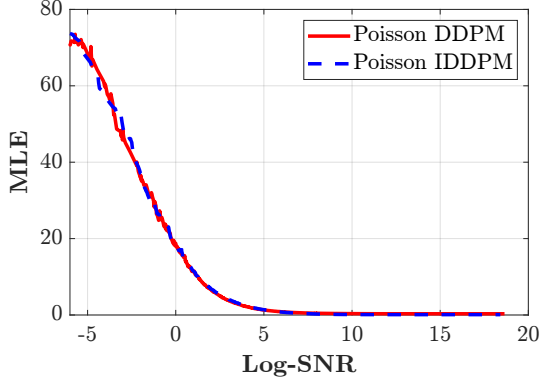


Figure 6. Test PRL versus logSNR values for Poisson diffusion models

Table 2. Negative Log-Likelihood (NLL), $\mathbb{E}[-\log P(x)]$ on LMD Music Test Data (bits per dimension)

Noise + Loss Function	NLL
Gaussian + MSE	0.51
ItDPDM: Poisson + PRL (ours)	4.61×10^{-5}

with IDDPM yielding slightly better results. This highlights ItDPDM’s efficacy for discrete non-negative distributions, achieving lower test NLL values than ITDiff and Gaussian + MSE, without requiring soft discretization or uniform dequantization.

Figures 5 and 6 compare the denoising performance across SNR values. Fig.5 shows the MSE on test data as a function of logSNR for ITDiff and Gaussian + MSE models, while Fig.6 presents the PRL-based denoising for ItDPDM. Notably, PRL values at low SNRs are significantly lower than the corresponding MSE values for Gaussian models, aligning with the test NLL improvements in Table 1. Similar trends are observed in Table 2, which compares test NLL results on symbolic music data. The NLL gap is even more pronounced, underscoring ItDPDM’s suitability for discrete data generation and affirming the suitability of ItDPDM with PRL loss for these tasks.

6.4. Cross Training Paradigm

To evaluate the poisson reconstruction loss (PRL) for discrete denoising, we apply cross-training, training a Gaussian diffusion model with PRL (**Gaussian + PRL**) and a Poisson diffusion model with MSE (**Poisson + MSE**). Table 1 reports test NLL values. First, Poisson diffusion performs better with PRL (ItDPDM) than with MSE, confirming PRL’s suitability for Poisson models. Second, Gaussian diffusion also benefits from PRL, as Gaussian + PRL outperforms Gaussian + MSE. These results suggest that PRL is superior for discrete data modeling, consistently outperforming MSE

in both Gaussian and Poisson noise schemes.

Additionally, we observe that the proposed method converges: a) much faster and b) to a lower loss than the Gaussian baseline in both the cases, as illustrated in Figure 7. To empirically validate our **exact** I-MPRL identity, we compare the area under the per-logSNR loss curves (Figures 5, 6) with the asymptotic average training losses in Figure 7. Across both Gaussian and Poisson noise models, we observe a remarkably tight numerical correspondence between these quantities, as predicted by our theoretical framework.

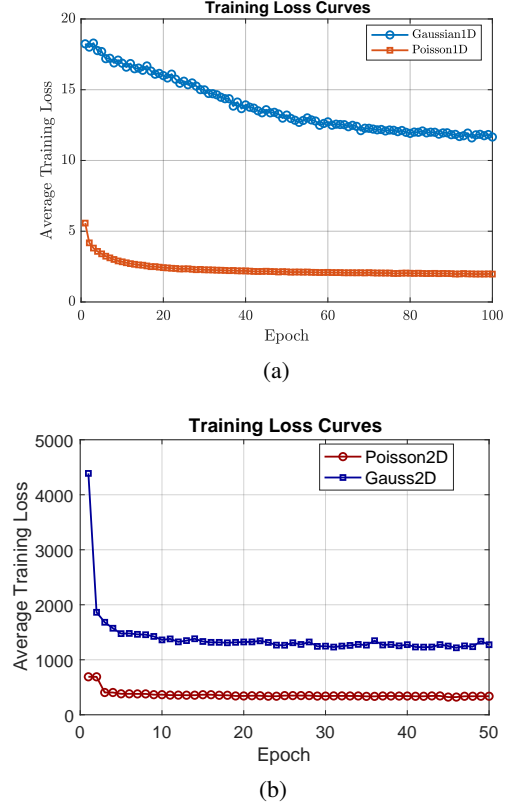


Figure 7. Comparing convergence speeds in 1D/2D cases Gaussian & Poisson

7. Related Work

The success of diffusion models extends to restoration tasks like inpainting and super-resolution (Nichol & Dhariwal, 2021; Lugmayr et al., 2022), underscoring their versatility. Mathematically, these models are grounded in denoising autoencoders (Vincent, 2011), variational inference (Kingma et al., 2021), and score-based stochastic differential equations (Song et al., 2020), with recent advances formalizing their information-theoretic foundations (Kong et al., 2023). Theoretical advancements continue to refine these frameworks. Annealed score matching (Hyvärinen, 2005; Song & Ermon, 2019) and stochastic differential equations (SDEs) (Song et al., 2020) have generalized diffusion processes to non-Gaussian settings, while SDE-based formula-

tions (Dockhorn et al., 2022) formalize convergence properties. Recent information-theoretic perspectives (Kong et al., 2023) unify these approaches by linking mutual information and minimum mean squared error (MMSE) (Guo et al., 2005), enabling exact likelihood bounds for Gaussian diffusion.

8. Conclusion

We propose ItDPDM, a novel discrete Poisson diffusion model enhanced by the PRL objective. By deriving exact information-theoretic relations, we improve diffusion training, achieving lower negative log likelihoods than existing models. Our framework extends Poisson noise modeling to discrete data generation, without requiring continuous approximations. Future work can explore broader applications in symbolic music and other structured data domains.

References

- Abramowitz, M. and Stegun, I. A. *Handbook of Mathematical Functions with Formulas, Graphs, and Mathematical Tables*. Dover Publications, 1964.
- Atar, R. and Weissman, T. Mutual information, relative entropy, and estimation in the poisson channel, 2010. URL <https://arxiv.org/abs/1101.0302>.
- Austin, J., Johnson, D., Ho, J., Tarlow, D., van den Berg, R., and Abbeel, P. Structured denoising diffusion models in discrete state-spaces. *Advances in Neural Information Processing Systems*, 34:17981–17993, 2021.
- Avrahami, O., Bar-Tal, O., Shahar, S., Benaim, S., and Hassner, T. Retrieve first, generate later: Towards retrieval-augmented text-to-image generation. *arXiv preprint arXiv:2209.15189*, 2022.
- Banerjee, A., Guo, X., and Wang, H. On the optimality of conditional expectation as a bregman predictor. *IEEE Transactions on Information Theory*, 51(7):2664–2669, 2005. doi: 10.1109/TIT.2005.850145.
- Bar-David, I. Communication under the poisson regime. *IEEE Transactions on Information Theory*, 15(1):31–37, 1969. doi: 10.1109/TIT.1969.1054238.
- Bishop, C. M. *Pattern Recognition and Machine Learning*. Springer, 2006.
- Braiman, V., Malyarenko, A., Mishura, Y., and Rudyk, Y. A. Properties of shannon and rényi entropies of the poisson distribution as the functions of intensity parameter, 2024. URL <https://arxiv.org/abs/2403.08805>.
- Brekelmans, R., Masrani, V., Wood, F., Steeg, G. V., and Galstyan, A. All in the exponential family: Bregman duality in thermodynamic variational inference, 2020. URL <https://arxiv.org/abs/2007.00642>.
- Chen, N., Zhang, Y., Zen, H., Weiss, R. J., Norouzi, M., Dehak, N., and Chan, W. Wavegrad 2: Iterative refinement for text-to-speech synthesis, 2021. URL <https://arxiv.org/abs/2106.09660>.
- Chen, T. and Zhou, M. Learning to jump: Thinning and thickening latent counts for generative modeling, 2023. URL <https://arxiv.org/abs/2305.18375>.
- Chernoff, H. *Measure of Asymptotic Efficiency for Statistical Tests*. Annals of Mathematical Statistics, 1952.
- Davis, M. *Markov Models and Optimization*. Chapman & Hall, 1993.
- Dhariwal, P. and Nichol, A. Q. Diffusion models beat gans on image synthesis. *Advances in Neural Information Processing Systems*, 34:8780–8794, 2021.
- Diaconis, P. and Ylvisaker, D. Conjugate priors for exponential families. *The Annals of Statistics*, 7(2):269–281, 1979. ISSN 00905364, 21688966. URL <http://www.jstor.org/stable/2958808>.
- Dockhorn, T., Chung, H., Ermon, S., and Rätsch, G. Score-based generative models for high-dimensional inverse problems. *Advances in Neural Information Processing Systems*, 35:17506–17518, 2022.
- Duncan, T. On the calculation of mutual information. *SIAM Journal on Applied Mathematics*, 1970.
- Dupuis, P. and Ellis, R. S. The large deviation principle for a general class of queueing systems i. *Transactions of the American Mathematical Society*, 347(8):2689–2751, 1995. ISSN 00029947. URL <http://www.jstor.org/stable/2154753>.
- Dytso, A. and Vincent Poor, H. Estimation in poisson noise: Properties of the conditional mean estimator. *IEEE Transactions on Information Theory*, 66(7):4304–4323, 2020. doi: 10.1109/TIT.2020.2979978.
- Gelman, A. and Meng, X.-L. Simulating normalizing constants: From importance sampling to bridge sampling to path sampling. *Statistical Science*, 13(2):163–185, 1998. ISSN 08834237, 21688745. URL <http://www.jstor.org/stable/2676756>.
- Good, I. J. The population frequencies of species and the estimation of population parameters. *Biometrika*, 40(3-4): 237–264, 1953.
- Guo, D., Shamaï, S., and Verdú, S. Mutual information and minimum mean-square error in gaussian channels. *IEEE Transactions on Information Theory*, 51(4):1261–1282, 2005.

- Ho, J., Jain, A., and Abbeel, P. Denoising diffusion probabilistic models. *Advances in Neural Information Processing Systems*, 33:6840–6851, 2020.
- Ho, J., Saharia, C., Chan, W., Saxena, S., Srinivas, A., Ghasemipour, S. K. S., Lopes, R., Hu, H., Barzelay, A., Gontijo-Lopes, R., et al. Imagen video: High definition video generation with diffusion models. *arXiv preprint arXiv:2210.02303*, 2022.
- Hoogeboom, E. et al. Categorical diffusion with gumbel-softmax. *arXiv preprint arXiv:2107.08447*, 2021. URL <https://arxiv.org/abs/2107.08447>.
- Hyvärinen, A. Estimating the gradients of the log-density. In *Advances in Neural Information Processing Systems (NeurIPS)*, 2005. URL <https://papers.nips.cc/paper/2005>.
- Jing, B., Eismann, J. S., Satorras, V. G., and Fuchs, F. B. Torsional diffusion for molecular conformer generation. *arXiv preprint arXiv:2206.01729*, 2022.
- Kingma, D. P., Salimans, T., Ho, J., and Chen, X. Variational diffusion models. *Advances in Neural Information Processing Systems*, 34:21696–21707, 2021.
- Kong, X., Brekelmans, R., and Steeg, G. V. Information-theoretic diffusion, 2023. URL <https://arxiv.org/abs/2302.03792>.
- Kong, Z., Ping, W., Huang, J., Zhao, K., and Catanzaro, B. Diffwave: A versatile diffusion model for audio synthesis. *arXiv preprint arXiv:2009.09761*, 2021.
- Krizhevsky, A. Learning multiple layers of features from tiny images. <https://www.cs.toronto.edu/~kriz/cifar.html>, 2009.
- Liptser, R. S. and Shirayayev, A. N. *Statistics of Random Processes II: Applications*, volume 6 of *Applications of Mathematics*. Springer, Berlin, Heidelberg, 2nd edition, 2001. ISBN 978-3-540-21292-6. doi: 10.1007/978-3-662-04574-4. Part of the Stochastic Modelling and Applied Probability series.
- Lugmayr, A., Danelljan, M., Romero, A., Yu, F., Timofte, R., and Van Gool, L. Repaint: Inpainting using denoising diffusion probabilistic models. *Proceedings of the IEEE/CVF Conference on Computer Vision and Pattern Recognition*, pp. 11461–11471, 2022.
- Miller, K. S. *Mathematical Statistics: Basic Ideas and Selected Topics*. Pearson Education, 2nd edition, 2006. ISBN 9780131520780.
- Mulyukov, Z., Dinsdale, G., Glocker, B., and Schaap, M. Medical diffusion: Denoising diffusion probabilistic models for 3d medical image generation. *arXiv preprint arXiv:2211.02386*, 2022.
- Nguyen, C. M., Chan, E. R., Bergman, A. W., and Wetzstein, G. Diffusion in the dark: A diffusion model for low-light text recognition, 2023. URL <https://arxiv.org/abs/2303.04291>.
- Nichol, A. Q. and Dhariwal, P. Improved denoising diffusion probabilistic models. *International Conference on Machine Learning*, pp. 8162–8171, 2021.
- Ogata, Y. A monte carlo method for high dimensional integration. *Numer. Math.*, 55(2):137–157, March 1989. ISSN 0029-599X. doi: 10.1007/BF01406511. URL <https://doi.org/10.1007/BF01406511>.
- Plasser, M., Peter, S., and Widmer, G. Discrete diffusion probabilistic models for symbolic music generation, 2023. URL <https://arxiv.org/abs/2305.09489>.
- Ramesh, A., Pavlov, M., Goh, G., Gray, S., Voss, C., Radford, A., Chen, M., and Sutskever, I. Hierarchical text-conditional image generation with clip latents. *arXiv preprint arXiv:2204.06125*, 2022.
- Robbins, H. An empirical bayes approach to statistics. In *Proceedings of the Third Berkeley Symposium on Mathematical Statistics and Probability*, volume 1, pp. 157–163. University of California Press, 1956.
- Rombach, R., Blattmann, A., Lorenz, D., Esser, P., and Ommer, B. High-resolution image synthesis with latent diffusion models. *Proceedings of the IEEE/CVF Conference on Computer Vision and Pattern Recognition*, pp. 10684–10695, 2022.
- Ronneberger, O., Fischer, P., and Brox, T. U-net: Convolutional networks for biomedical image segmentation. *ArXiv*, abs/1505.04597, 2015. URL <https://api.semanticscholar.org/CorpusID:3719281>.
- Saharia, C., Chan, W., Saxena, S., Li, L., Whang, J., Denton, E., Ghasemipour, S. K. S., Ayan, B. K., Mahdavi, S., Lopes, R., et al. Imagen: Text-to-image diffusion models with unprecedented photorealism. *Advances in Neural Information Processing Systems*, 35:12302–12314, 2022a.
- Saharia, C., Chan, W., Saxena, S., Li, L., Whang, J., Denton, E., Ghasemipour, S. K. S., Ayan, B. K., Mahdavi, S., Lopes, R., et al. Photorealistic text-to-image diffusion models with deep language understanding. *Advances in Neural Information Processing Systems*, 35:12302–12314, 2022b.
- Shamai, S. and Wyner, A. A binary analog to the entropy-power inequality. *IEEE Transactions on Information Theory*, 36(6):1428–1430, 1990. doi: 10.1109/18.59938.
- Snyder, D. Filtering and detection for doubly stochastic poisson processes. *IEEE Transactions on Information Theory*, 1972.

- Song, Y. and Ermon, S. Generative modeling by estimating gradients of the data distribution. In *Proceedings of the 32nd Conference on Neural Information Processing Systems (NeurIPS 2019)*, 2019. URL <https://papers.nips.cc/paper/2019>.
- Song, Y., Sohl-Dickstein, J., Kingma, D. P., Kumar, A., Ermon, S., and Poole, B. Score-based generative modeling through stochastic differential equations. *arXiv preprint arXiv:2011.13456*, 2020.
- Trippe, B. L., Baker, D., Barzilay, R., and Jaakkola, T. Diffusion probabilistic modeling of protein backbones in 3d for the motif-scaffolding problem. *arXiv preprint arXiv:2206.04119*, 2022.
- Vaswani, A., Shazeer, N., Parmar, N., Uszkoreit, J., Jones, L., Gomez, A. N., Kaiser, Ł., and Polosukhin, I. Attention is all you need. In *Advances in Neural Information Processing Systems*, pp. 5998–6008, 2017.
- Verdú, S. Poisson communication theory. 2004. URL <https://api.semanticscholar.org/CorpusID:2997862>.
- Vincent, P. A connection between score matching, denoising autoencoders and density estimation. *Advances in Neural Information Processing Systems*, 24, 2011.
- Vogl, C., Ranzijn, J., Millwood, I., and Essl, G. The lakh midi dataset. <https://colinraffel.com/projects/lmd/>, 2017.
- Wang, L., Rodrigues, M., and Carin, L. Generalized bregman divergence and gradient of mutual information for vector poisson channels. In *2013 IEEE International Symposium on Information Theory*, pp. 454–458, 2013. doi: 10.1109/ISIT.2013.6620267.
- Weissman, T., Ordentlich, E., Seroussi, G., Verdú, S., and Weinberger, M. J. Universal discrete denoising: Known channel. *IEEE Transactions on Information Theory*, 51(1):5–28, 2005.

Appendix

A. Section 3 Proofs

A.1. On the Poisson Loss Function:

Here, as outlined in 3.2, we establish that the function $l_0(x) = x \log x - x + 1$ serves as the convex conjugate of the Poisson distribution's log moment generating function (log MGF). We begin by deriving the log MGF of the Poisson distribution, and finally computing its convex conjugate through the Legendre-Fenchel transform. Let X be a random variable following a Poisson distribution with parameter $\lambda > 0$. The probability mass function (PMF) of X is given by:

$$P(X = k) = \frac{\lambda^k e^{-\lambda}}{k!}, \quad \text{for } k = 0, 1, 2, \dots$$

The moment generating function (MGF) can be evaluated as:

$$M_X(t) = E[e^{tX}] = \sum_{k=0}^{\infty} e^{tk} P(X = k) = \sum_{k=0}^{\infty} e^{tk} \frac{\lambda^k e^{-\lambda}}{k!} = e^{-\lambda} \sum_{k=0}^{\infty} \frac{(\lambda e^t)^k}{k!} = e^{-\lambda} e^{\lambda e^t} = e^{\lambda(e^t - 1)}$$

Let $\phi(t)$ be the log moment generating function as shown:

$$\phi(t) = \log M_X(t) = \lambda(e^t - 1)$$

Without any loss of generality, let $\lambda = 1$ (since scaling does not affect the form of the conjugate), implying $\phi(t) = e^t - 1$. The **convex conjugate** of a convex function $\phi : \mathbb{R} \rightarrow \mathbb{R} \cup \{+\infty\}$, denoted by $\phi^*(x)$, is defined as:

$$\phi^*(x) = \sup_{t \in \mathbb{R}} \{xt - \phi(t)\}$$

This transformation maps the original function $\phi(t)$ to its dual function $\phi^*(x)$, and then finds the supremum of linear functions subtracted by $\phi(t)$.

Let $\phi(t) = e^t - 1$ be the log moment generating function (log MGF) of a Poisson distribution with parameter $\lambda = 1$. Then, the convex conjugate of ϕ , denoted by $\phi^*(x)$, is given by:

$$\phi^*(x) = \begin{cases} x \log x - x + 1 & \text{if } x > 0, \\ +\infty & \text{otherwise.} \end{cases}$$

Proof. By definition: $\phi^*(x) = \sup_{t \in \mathbb{R}} \{xt - \phi(t)\} = \sup_{t \in \mathbb{R}} \{xt - e^t + 1\}$

To find the supremum, we find the value of t that maximizes this expression. First-order conditions imply: $\frac{d}{dt} (xt - e^t) = x - e^t = 0$ so we have $t = \log x$. This critical point exists only if $x > 0$, as $e^t > 0$ for all $t \in \mathbb{R}$.

From the second-order condition, we get

$$\frac{d^2}{dt^2} (xt - e^t) = -e^t < 0 \quad \forall t \in \mathbb{R}$$

The negative second derivative confirms that the function is concave at $t = \log x$, ensuring a global maximum at this point.

So for $t = \log x$,

$$\phi^*(x) = x(\log x) - e^{\log x} + 1 = x \log x - x + 1$$

Therefore, for $x > 0$:

$$\phi^*(x) = x \log x - x + 1$$

For $x \leq 0$, the supremum is unbounded above, leading to: $\phi^*(x) = +\infty$ Combining these cases gives:

$$\phi^*(x) = \begin{cases} x \log x - x + 1 & \text{if } x > 0, \\ +\infty & \text{otherwise.} \end{cases}$$

This establishes that $l_0(x) = x \log x - x + 1$ is the convex conjugate of the Poisson distribution's log moment generating function $\phi(t) = e^t - 1$ and therefore, a natural loss function.

CONNECTION TO BREGMAN DIVERGENCE

The Poisson loss function we defined $l(x, \hat{x})$ is a member of the broader family of Bregman divergences, which are pivotal in various domains such as machine learning, information theory, and optimization. A Bregman divergence is defined for a strictly convex and differentiable function $\psi : \mathbb{R}^d \rightarrow \mathbb{R}$ as follows:

$$\mathcal{L}_\psi(x, \hat{x}) = \psi(x) - \psi(\hat{x}) - \langle \nabla \psi(\hat{x}), x - \hat{x} \rangle,$$

where $\langle \cdot, \cdot \rangle$ denotes the inner product in \mathbb{R}^d , and $\nabla \psi(\hat{x})$ represents the gradient of ψ evaluated at \hat{x} .

For the Poisson loss function, the generating function ψ is chosen as:

$$\psi(x) = x \log x - x.$$

Substituting this into the Bregman divergence definition yields:

$$\mathcal{L}_\psi(x, \hat{x}) = x \log x - x - (\hat{x} \log \hat{x} - \hat{x}) - (\log \hat{x} \cdot (x - \hat{x})).$$

Simplifying the expression, we obtain:

$$\mathcal{L}_\psi(x, \hat{x}) = x \log \left(\frac{x}{\hat{x}} \right) - x + \hat{x},$$

which is precisely the Poisson loss function $l(x, \hat{x})$.

This framework not only encapsulates the Poisson loss but also generalizes it to encompass other widely-used loss functions by merely altering the generating function ψ . Well-known examples include squared error loss (choosing $\psi(x) = \frac{1}{2}x^2$ and Itakura-Saito divergence (choosing $\psi(x) = -\log x$). Bregman divergences exhibit key properties that make them valuable in optimization and learning. They are **non-negative**, vanishing only when $x = \hat{x}$, due to the strict convexity of ψ . They are also **asymmetric**, meaning $\mathcal{L}_\psi(x, \hat{x}) \neq \mathcal{L}_\psi(\hat{x}, x)$ in general and their **projection property** enables efficient optimization over convex sets.

By leveraging the Bregman divergence framework, Poisson and Gaussian diffusion schemes can be unified under a single theoretical umbrella, where squared error loss ($\psi(x) = \frac{1}{2}x^2$) corresponds to Gaussian noise, and Poisson loss aligns with count-based data modeling. This unification enables extending optimization techniques across different noise models by adjusting the generating function ψ . Viewing Poisson loss function as a Bregman divergence thus broadens its theoretical and practical utility discrete data modelling.

OPTIMALITY OF CONDITIONAL EXPECTATION

Let $\phi : \mathbb{R}^d \rightarrow \mathbb{R}$ be a strictly convex and differentiable function. The Bregman divergence D_ϕ induced by ϕ is defined by

$$D_\phi(x, y) = \phi(x) - \phi(y) - \nabla \phi(y)^\top (x - y).$$

Consider a random variable $X \in \mathbb{R}^d$ and a sigma-algebra $\sigma(Z)$ with $Y = Y(Z)$ being any measurable function of Z . Let $Y^* = E[X|Z]$ denote the conditional expectation of X given Z . The objective is to show that Y^* uniquely minimizes the expected Bregman loss $E[D_\phi(X, Y)]$ among all measurable functions $Y(Z)$.

For any such function Y , consider the difference in expected Bregman losses:

$$E[D_\phi(X, Y)] - E[D_\phi(X, Y^*)] = E[\phi(X) - \phi(Y) - \nabla \phi(Y)^\top (X - Y)] - E[\phi(X) - \phi(Y^*) - \nabla \phi(Y^*)^\top (X - Y^*)].$$

Simplifying, the terms involving $\phi(X)$ cancel out, yielding

$$E[D_\phi(X, Y)] - E[D_\phi(X, Y^*)] = E[\phi(Y^*) - \phi(Y) - \nabla \phi(Y)^\top (Y^* - Y)].$$

Recognizing that Y^* is the conditional expectation $E[X|Z]$, we utilize the law of total expectation to express the above as

$$E[\phi(Y^*) - \phi(Y) - \nabla \phi(Y)^\top (Y^* - Y)] = E[D_\phi(Y^*, Y)].$$

Due to the strict convexity of ϕ , the Bregman divergence satisfies $D_\phi(u, v) \geq 0$ for all $u, v \in \mathbb{R}^d$, with equality if and only if $u = v$. Therefore,

$$E[D_\phi(X, Y)] - E[D_\phi(X, Y^*)] = E[D_\phi(Y^*, Y)] \geq 0,$$

with equality holding if and only if $Y = Y^*$ almost surely. This establishes that

$$E[D_\phi(X, Y)] \geq E[D_\phi(X, Y^*)],$$

for all measurable functions $Y(Z)$, and thus $Y^* = E[X|Z]$ is the unique minimizer of the expected Bregman loss $E[D_\phi(X, Y)]$.

A.2. Section 3 Lemma Proofs

Proof of Lemma 3.1: Properties of Poisson Loss Consider the loss function defined as $l(x, \hat{x}) = \hat{x} \cdot l_0\left(\frac{x}{\hat{x}}\right)$, where $l_0(z) = z \log z - z + 1$.

1. Non-negativity: Since $l_0(z)$ achieves its minimum value of 0 at $z = 1$ and is non-negative for all $z > 0$, it follows that $l(x, \hat{x}) \geq 0$ for all $x, \hat{x} > 0$. Equality holds if and only if $\frac{x}{\hat{x}} = 1$, i.e., $x = \hat{x}$.

2. Convexity: The function $l_0(z)$ is convex in z because its second derivative $l_0''(z) = \frac{1}{z}$ is positive for all $z > 0$. Therefore, $l(x, \hat{x}) = \hat{x} \cdot l_0\left(\frac{x}{\hat{x}}\right)$ is convex in \hat{x} for each fixed x , and similarly, it is convex in x for each fixed \hat{x} , as the composition of a convex function with an affine transformation preserves convexity. (We can also directly use the Bregman divergence framework to argue its convexity)

3. Scaling: For any $\alpha > 0$, consider scaling both arguments of the loss function:

$$l(\alpha x, \alpha \hat{x}) = \alpha \hat{x} \cdot l_0\left(\frac{\alpha x}{\alpha \hat{x}}\right) = \alpha \hat{x} \cdot l_0\left(\frac{x}{\hat{x}}\right) = \alpha \cdot l(x, \hat{x}).$$

This demonstrates that the loss function scales linearly with α .

4. Unboundedness for Underestimation: For any fixed $x > 0$, as $\hat{x} \rightarrow 0^+$, the ratio $\frac{x}{\hat{x}} \rightarrow \infty$. Evaluating the loss function in this limit:

$$l(x, \hat{x}) = \hat{x} \cdot \left(\frac{x}{\hat{x}} \log\left(\frac{x}{\hat{x}}\right) - \frac{x}{\hat{x}} + 1 \right) = x \log\left(\frac{x}{\hat{x}}\right) - x + \hat{x}.$$

As $\hat{x} \rightarrow 0^+$, $\log\left(\frac{x}{\hat{x}}\right)$ grows without bound, causing $l(x, \hat{x}) \rightarrow \infty$. This shows that the loss becomes unbounded as \hat{x} underestimates x .

Proof of Lemma 3.2. Let Z_γ be a Poisson random variable with parameter γX , meaning $Z_\gamma|X = x \sim \text{Pois}(\gamma x)$. Suppose the conditional expectation $\langle X \rangle_z = E[X|Z_\gamma = z]$ is affine in z ,

$$\langle X \rangle_z = az + b,$$

for some a and b , with $0 < a < 1/\gamma$ and $b > 0$. We aim to show that X follows a Gamma distribution with shape $\alpha = \frac{1-\gamma a}{a}$ and rate $\beta = \frac{a}{b}$, i.e.,

$$X \sim \text{Gamma}\left(\frac{1-\gamma a}{a}, \frac{a}{b}\right).$$

Define $U = X$ and $Y = Z_\gamma \sim \mathcal{P}(\gamma U)$. Assume $E[U|Y = z] = az + b$. By the law of total expectation,

$$0 = E[(U - (aY + b))g(Y)]$$

for any function g satisfying integrability. Choosing $g(Y) = e^{-tY}$ for $t > 0$,

$$E[(U - (aY + b))e^{-tY}] = 0.$$

Rewriting $Y \sim \mathcal{P}(\gamma U)$, we use the known conditional Laplace transform relation for a $\mathcal{P}(\lambda)$ random variable Y ,

$$E[e^{-tY}|U = u] = \exp(u(\gamma(e^{-t} - 1))).$$

Hence,

$$E[e^{-tY}] = E[\exp(U\gamma(e^{-t} - 1))],$$

which is the Laplace transform of U evaluated at $s = \gamma(1 - e^{-t})$. Denote

$$L_U(s) = E[e^{-sU}], \quad \text{so that} \quad E[e^{-tY}] = L_U(\gamma(1 - e^{-t})).$$

Similarly,

$$E[Ue^{-tY}] = -\frac{d}{ds}L_U(s)\Big|_{s=\gamma(1-e^{-t})}, \quad E[Ye^{-tY}] = -\frac{d}{dt}E[e^{-tY}].$$

From the orthogonality condition,

$$E[(U - (aY + b))e^{-tY}] = 0.$$

Using the above expressions,

$$0 = E[Ue^{-tY}] - aE[Ye^{-tY}] - bE[e^{-tY}].$$

Substituting $s = \gamma(1 - e^{-t})$ and differentiating as needed, we obtain a first-order linear differential equation for $L_U(s)$,

$$-((1 - a\gamma) + a\gamma s)L'_U(s) = bL_U(s).$$

The unique solution with $L_U(0) = 1$ is

$$L_U(s) = \left(1 + \frac{b}{1 - \gamma a}s\right)^{-\frac{1 - \gamma a}{a}}.$$

This is the Laplace transform of a $\text{Gamma}(\frac{1 - \gamma a}{a}, \frac{a}{b})$ random variable. Hence, $U = X$ follows this Gamma distribution. For the Gamma distribution to be well-defined with a positive shape parameter, we require $\alpha = \frac{1 - \gamma a}{a} > 0$, which holds for $0 < a < \frac{1}{\gamma}$. The rate parameter $\beta = \frac{a}{b} > 0$ requires $b > 0$. Under these conditions, $X \sim \text{Gam}(\frac{1 - \gamma a}{a}, \frac{a}{b})$, completing the proof.

Proof of Lemma 3.4. Consider $Z_\gamma = \mathcal{P}(\gamma X)$, where Z_γ is a Poisson random variable with parameter γX . To determine $\langle X \rangle_z = E[X|Z_\gamma = z]$ for each $z \geq 0$, we start by applying the definition of conditional expectation:

$$\langle X \rangle_z = \frac{E[X \cdot P_{Z_\gamma}(z|X)]}{P_{Z_\gamma}(z)}.$$

Given that $Z_\gamma|X = x \sim \text{Pois}(\gamma x)$, the conditional probability mass function is

$$P_{Z_\gamma}(z|X = x) = \frac{(\gamma x)^z e^{-\gamma x}}{z!}.$$

Substituting this into the expression for $\langle X \rangle_z$ yields

$$\langle X \rangle_z = \frac{E\left[X \cdot \frac{(\gamma X)^z e^{-\gamma X}}{z!}\right]}{P_{Z_\gamma}(z)}.$$

To relate $\langle X \rangle_z$ to $P_{Z_\gamma}(z + 1)$, observe that

$$P_{Z_\gamma}(z + 1) = E\left[\frac{(\gamma X)^{z+1} e^{-\gamma X}}{(z + 1)!}\right] = \frac{\gamma}{z + 1} E\left[X \cdot \frac{(\gamma X)^z e^{-\gamma X}}{z!}\right].$$

Rearranging the above equation, we obtain

$$E\left[X \cdot \frac{(\gamma X)^z e^{-\gamma X}}{z!}\right] = \frac{(z + 1)}{\gamma} P_{Z_\gamma}(z + 1).$$

Substituting this back into the expression for $\langle X \rangle_z$, we have

$$\langle X \rangle_z = \frac{\frac{(z+1)}{\gamma} P_{Z_\gamma}(z+1)}{P_{Z_\gamma}(z)} = \frac{1}{\gamma} \frac{(z+1) P_{Z_\gamma}(z+1)}{P_{Z_\gamma}(z)}.$$

This completes the proof of Lemma 3.4.

Proof of Lemma 3.5. Let $Z_\gamma = \mathcal{P}(\gamma X)$. We claim that for every positive integer k and nonnegative integer z ,

$$E[(\gamma X)^k | Z_\gamma = z] = \prod_{i=0}^{k-1} E[\gamma X | Z_\gamma = z + i].$$

From the affine formula in Lemma 3.4, the conditional expectation of γX given $Z_\gamma = z$ is related to the ratio of marginal probabilities. More generally, for higher-order moments,

$$E[(\gamma X)^k | Z_\gamma = z] = \frac{(z+k)!}{z!} \frac{P_{Z_\gamma}(z+k)}{P_{Z_\gamma}(z)}. \quad (31)$$

We can also express $(\gamma X)^k$ as a product of γX terms and use the Poisson shifting property of $\mathcal{P}(\gamma X)$. Applying Lemma 3.4 and (31) for each shift $z \rightarrow z + i$ gives

$$E[(\gamma X)^k | Z_\gamma = z] = \prod_{i=0}^{k-1} E[\gamma X | Z_\gamma = z + i].$$

Each factor on the right captures the conditional expectation of γX at consecutive levels $z, z+1, \dots, z+k-1$, so all higher-order moments of γX follow from the first conditional moment $E[\gamma X | Z_\gamma = z]$. This completes the proof.

Proof Sketch of 31: The key observation behind the formula is that, for the Poisson distribution, shifting from y to $y+k$ multiplies the corresponding probability mass by $\frac{(aX+\lambda)^k}{k!}$. Evaluating the expectation leverages the ratio of adjacent Poisson probabilities $P_Y(y+k)/P_Y(y)$ and tracks how $(aX+\lambda)^k$ factors. In essence, a product expansion shows how each additional factor $aX + \lambda$ increases the count from y to $y+1$, and iterating this argument recovers the moment expression.

Proof of Lemma 3.6. Let $Z_\gamma = \mathcal{P}(\gamma X)$, where Z_γ is a Poisson random variable with parameter γX . We first compute the derivative of the conditional probability mass function $P_{Z_\gamma}(z | X = x)$ with respect to γ .

Since Z_γ given $X = x$ follows a Poisson distribution with mean γx , we have

$$P_{Z_\gamma}(z | X = x) = \frac{(\gamma x)^z e^{-\gamma x}}{z!}.$$

Taking the derivative with respect to γ and using product rule, we obtain:

$$\frac{d}{d\gamma} P_{Z_\gamma}(z | X = x) = \frac{d}{d\gamma} \left(\frac{(\gamma x)^z e^{-\gamma x}}{z!} \right) = \frac{z(\gamma x)^{z-1} x e^{-\gamma x}}{z!} - \frac{x(\gamma x)^z e^{-\gamma x}}{z!}.$$

Simplifying the terms, we obtain

$$\frac{d}{d\gamma} P_{Z_\gamma}(z | X = x) = x \left(\frac{(\gamma x)^{z-1} e^{-\gamma x}}{(z-1)!} - \frac{(\gamma x)^z e^{-\gamma x}}{z!} \right).$$

Notice that

$$\frac{(\gamma x)^{z-1} e^{-\gamma x}}{(z-1)!} = P_{Z_\gamma}(z-1 | X = x),$$

we can rewrite the derivative as

$$\frac{d}{d\gamma} P_{Z_\gamma}(z | X = x) = x (P_{Z_\gamma}(z-1 | X = x) - P_{Z_\gamma}(z | X = x)).$$

This establishes the first part of the lemma.

Next, we compute the derivative of the marginal probability $P_{Z_\gamma}(z)$ with respect to γ . By the law of total probability, we have

$$P_{Z_\gamma}(y) = E [P_{Z_\gamma}(z | X)].$$

Differentiating both sides with respect to γ , we obtain

$$\frac{d}{d\gamma} P_{Z_\gamma}(z) = E \left[\frac{d}{d\gamma} P_{Z_\gamma}(z|X) \right].$$

Substituting the result from above, we get

$$\frac{d}{d\gamma} P_{Z_\gamma}(z) = E \left[x (P_{Z_\gamma}(z-1|X) - P_{Z_\gamma}(z|X)) \right].$$

This can be expressed as

$$\gamma \frac{d}{d\gamma} P_{Z_\gamma}(z) = \gamma E [x P_{Z_\gamma}(z-1|X)] - \gamma E [x P_{Z_\gamma}(z|X)].$$

Noting that for a Poisson distribution, $E [x P_{Z_\gamma}(z|X)] = \frac{z}{\gamma} P_{Z_\gamma}(z)$ and $E [x P_{Z_\gamma}(z-1|X)] = \frac{z}{\gamma} P_{Z_\gamma}(z)$, we substitute to obtain

$$\gamma \frac{d}{d\gamma} P_{Z_\gamma}(z) = z P_{Z_\gamma}(z) - (z+1) P_{Z_\gamma}(z+1).$$

Thus, the second part of the lemma is established.

OTHER PROPERTIES OF THE CONDITIONAL EXPECTATION

Theorem A.1. Let $Z_\gamma = \mathcal{P}(\gamma X)$ where X is a nonnegative random variable, and $\gamma > 0$. Then, for every $\gamma > 0$ and integer $z \geq 0$,

$$\frac{d}{d\gamma} E [X|Z_\gamma = z] = -z\gamma \text{Var} (X|Z_\gamma = z-1),$$

where $\text{Var} (X|Z_\gamma = -1) = 0$.

Proof. Fix an integer $z \geq 0$. Consider the conditional expectation

$$E [X|Z_\gamma = z] = \frac{1}{\gamma} \left((z+1) \frac{P(Z_\gamma = z+1)}{P(Z_\gamma = z)} \right).$$

Differentiating both sides with respect to γ , we obtain

$$\frac{d}{d\gamma} E [X|Z_\gamma = z] = \frac{1}{\gamma} \frac{d}{d\gamma} \left((z+1) \frac{P(Z_\gamma = z+1)}{P(Z_\gamma = z)} \right) - \frac{1}{\gamma^2} \left((z+1) \frac{P(Z_\gamma = z+1)}{P(Z_\gamma = z)} \right).$$

Applying the quotient rule to the derivative inside the parentheses, we get

$$\frac{d}{d\gamma} \left(\frac{P(Z_\gamma = z+1)}{P(Z_\gamma = z)} \right) = \frac{P(Z_\gamma = z) \frac{d}{d\gamma} P(Z_\gamma = z+1) - P(Z_\gamma = z+1) \frac{d}{d\gamma} P(Z_\gamma = z)}{P(Z_\gamma = z)^2}.$$

Using the properties of the Poisson distribution, specifically the identity

$$\frac{P(Z_\gamma = z+1)}{P(Z_\gamma = z)} = \frac{\gamma X}{z+1},$$

we can simplify the derivative expression. Substituting back, we obtain

$$\frac{d}{d\gamma} E [X|Z_\gamma = z] = -z\gamma \text{Var} (X|Z_\gamma = z-1).$$

For the case $z = 0$, the derivative simplifies to $\frac{d}{d\gamma} E [X|Z_\gamma = 0] = 0$, since $\text{Var} (X|Z_\gamma = -1) = 0$ by definition.

The result for higher moments follows similarly. For any positive integer k , differentiating $E [(\gamma X)^k | Z_\gamma = z]$ with respect to γ and applying the quotient rule leads to the stated piecewise expression. This completes the proof.

Moreover, for any positive integer k ,

$$\frac{d}{d\gamma} E [(\gamma X)^k | Z_\gamma = z] = \begin{cases} k E [(\gamma X)^{k-1} | Z_\gamma = 0], & z = 0, \\ \frac{(z+k) E [(\gamma X)^{k-1} | Z_\gamma = z] E [\gamma X | Z_\gamma = z-1] - z E [(\gamma X)^k | Z_\gamma = z]}{E [\gamma X | Z_\gamma = z-1]}, & z \geq 1. \end{cases}$$

Theorem A.2. Let $Z_\gamma \sim \mathcal{P}(\gamma X)$. Then, for every fixed $\gamma > 0$ and any non-degenerate X , the mapping $z \mapsto E[X|Z_\gamma = z]$ is strictly increasing.

Proof. To show that $E[X|Z_\gamma = z]$ is strictly increasing, we define $U = \gamma X$ and consider the Poisson marginal probability:

$$P_{Z_\gamma}(k) = \frac{1}{k!} E[U^k e^{-U}]. \quad (32)$$

Applying the Cauchy-Schwarz inequality, we obtain

$$P_{Z_\gamma}(k) \leq \frac{1}{k!} \sqrt{E[U^{k+1} e^{-U}] E[U^{k-1} e^{-U}]}. \quad (33)$$

Rewriting in terms of factorial expressions, we get

$$P_{Z_\gamma}(k) \leq \sqrt{\frac{k+1}{k}} P_{Z_\gamma}(k+1) P_{Z_\gamma}(k-1). \quad (34)$$

Now, substituting this bound into the Turing-Good-Robbins (TGR) formula from Lemma 3.4:

$$E[U|Z_\gamma = z] = \frac{(z+1)P_{Z_\gamma}(z+1)}{P_{Z_\gamma}(z)}, \quad (35)$$

we obtain the lower bound

$$E[U|Z_\gamma = z] \geq \frac{(z+1) \frac{z}{z+1} P_{Z_\gamma}^2(z)}{P_{Z_\gamma}(z) P_{Z_\gamma}(z-1)}. \quad (36)$$

Simplifying, this reduces to

$$E[U|Z_\gamma = z] \geq \frac{z P_{Z_\gamma}(z)}{P_{Z_\gamma}(z-1)}. \quad (37)$$

Using the same formulation for $z-1$, we conclude

$$E[U|Z_\gamma = z] \geq E[U|Z_\gamma = z-1]. \quad (38)$$

Since $X = U/\gamma$, it follows that $E[X|Z_\gamma = z]$ is strictly increasing in z , completing the proof.

A.3. Incremental Channel Approach to I-MMLE and related proofs:

Here, we derive interesting relations between the mutual information in a Poisson noise channel and various parameters of the channel. The general distribution we consider here is $Y \sim \text{Poisson}(\alpha X + \lambda)$.

Theorem A.3. Let $\lambda > 0$ and let X be a positive random variable satisfying $E\{X \log X\} < \infty$. Consider the Poisson random transformation $X \mapsto Z_\lambda = \mathcal{P}(X + \lambda)$. Then, the derivative of the mutual information between X and Z_λ with respect to the dark current λ is given by

$$\frac{d}{d\lambda} I(X; Z_\lambda) = E[\log(X + \lambda) - \log\langle X + \lambda \rangle],$$

where $\langle X + \lambda \rangle = E[X + \lambda|Z_\lambda = z]$.

Proof: Let $Y_0 = \mathcal{P}(X)$ and $N_\lambda = \mathcal{P}(\lambda)$ be independent Poisson random variables with means X and λ , respectively. Define $Y_\lambda = Y_0 + N_\lambda$, which has the same distribution as $\mathcal{P}(X + \lambda)$. By the definition of mutual information,

$$I(X; Y_0) - I(X; Y_\lambda) = E\{L(X, Y_0, Y_\lambda)\},$$

where the expectation is over the joint distribution of (X, Y_0, Y_λ) , and the log-likelihood ratio is

$$L(x, k, \ell) = \log \frac{P_{Y_0|X}(k|x)}{P_{Y_0}(k)} - \log \frac{P_{Y_\lambda|X}(\ell|x)}{P_{Y_\lambda}(\ell)}.$$

Given that $Y_0|X = x \sim \mathcal{P}(x)$ and $Y_\lambda|X = x \sim \mathcal{P}(x + \lambda)$, the conditional probabilities are

$$P_{Y_0|X}(k|x) = \frac{x^k e^{-x}}{k!}, \quad P_{Y_\lambda|X}(\ell|x) = \frac{(x + \lambda)^\ell e^{-(x+\lambda)}}{\ell!}.$$

Substituting these into the log-likelihood ratio, we obtain

$$L(X, Y_0, Y_\lambda) = Y_0 \log X - Y_\lambda \log(X + \lambda) + U,$$

where U encompasses terms involving the logarithms of the marginal probabilities. Taking the expectation, we have

$$E[L] = E\{X \log X - (X + \lambda) \log(X + \lambda)\} + E[U].$$

Expanding $Y_\lambda = Y_0 + N_\lambda$ and leveraging the independence of N_λ from Y_0 , we analyze the behavior of $E[U]$ as λ becomes small. Through a series of manipulations and applying the dominated convergence theorem, we find that

$$I(X; Y_\lambda) - I(X; Y_0) = \lambda E \left[\log \frac{X}{\langle X \rangle} \right] + o(\lambda).$$

Dividing both sides by λ and taking the limit as $\lambda \rightarrow 0$, we obtain

$$\frac{d}{d\lambda} I(X; Y_\lambda) = E [\log(X + \lambda) - \log \langle X + \lambda \rangle],$$

where $\langle X + \lambda \rangle = E[X + \lambda | Y_\lambda = z]$. This completes the proof of Theorem A.3.

Theorem A.4. For every Poisson transformation \mathcal{P}_X with $E\{X \log X\} < \infty$, and as $\delta \rightarrow 0$,

$$I(X; \mathcal{P}((1 + \delta)X)) - I(X; \mathcal{P}(X)) = \delta E\{X \log X - \langle X \rangle \log \langle X \rangle\} + o(\delta).$$

Proof: Consider first the case $\delta \rightarrow 0^+$. Let $Y = \mathcal{P}(X)$ and $Z = \mathcal{P}(\delta X)$ be independent conditioned on X . Define $Y_\delta = Y + Z$. Then, the left-hand side of the lemma can be expressed as

$$I(X; Y_\delta) - I(X; Y) = E \left\{ \log \frac{P_{Y_\delta|X}(Y_\delta|X)}{P_{Y_\delta}(Y_\delta)} - \log \frac{P_{Y|X}(Y|X)}{P_Y(Y)} \right\}.$$

Expanding the log-likelihood ratio, we have

$$= E \left\{ Z \log X - \delta X - \log \frac{E\{(X')^{Y_\delta} e^{-(1+\delta)X'} | Y_\delta\}}{E\{(X')^Y e^{-X'} | Y\}} \right\}.$$

Here, X' is identically distributed as X but independent of Y and Z .

To analyze the expression as $\delta \rightarrow 0$, we approximate $\Delta = \mathcal{P}(\delta X)$ by a Bernoulli random variable that takes the value 1 with probability δX (conditioned on X) and 0 otherwise. This approximation is valid because for small δ , the Poisson distribution $\mathcal{P}(\delta X)$ closely resembles a Bernoulli distribution.

Substituting this approximation into the previous step, we obtain

$$I(X; Y_\delta) - I(X; Y) = E \left\{ Z \log X - \delta X - \log \left[(1 - \delta X) E\{(X')^Y e^{-X'} | Y\} + \delta X E\{(X')^{Y+1} e^{-X'} e^{-\delta X'} | Y\} \right] \right\} + o(\delta) \quad (39)$$

Expanding $e^{-\delta X'}$ to first order in δ , we have $e^{-\delta X'} \approx 1 - \delta X'$. Therefore,

$$E\{(X')^{Y+1} e^{-X'} e^{-\delta X'} | Y\} \approx E\{(X')^{Y+1} e^{-X'} | Y\} - \delta E\{(X')^{Y+2} e^{-X'} | Y\} + o(\delta) \quad (40)$$

Substituting this back into the logarithm and applying the first-order Taylor expansion $\log(1 + \epsilon) \approx \epsilon$ for small ϵ , we obtain

$$\begin{aligned} & \log \left[(1 - \delta X) E\{(X')^Y e^{-X'} | Y\} + \delta X E\{(X')^{Y+1} e^{-X'} | Y\} \right] \\ & \approx \log \left[E\{(X')^Y e^{-X'} | Y\} \right] + \frac{\delta X E\{(X')^{Y+1} e^{-X'} | Y\} - \delta X E\{(X')^Y e^{-X'} | Y\}}{E\{(X')^Y e^{-X'} | Y\}} + o(\delta) \\ & = \log \langle X \rangle - \delta X \frac{E\{(X')^Y e^{-X'} | Y\} - E\{(X')^{Y+1} e^{-X'} | Y\}}{E\{(X')^Y e^{-X'} | Y\}} + o(\delta), \end{aligned}$$

where $\langle X \rangle = E\{X|Y\}$.

Substituting this approximation back into equation 39, we get

$$I(X; Y_\delta) - I(X; Y) = E \left\{ Z \log X - \delta X - \log \langle X \rangle + \delta X \frac{E\{(X')^{Y+1} e^{-X'} | Y\}}{E\{(X')^Y e^{-X'} | Y\}} \right\} + o(\delta) \quad (41)$$

Noting that Z is Poisson with parameter X , we have $E\{Z|X\} = X$, and thus $E\{Z \log X\} = E\{X \log X\}$.

Furthermore, we know that $\langle X \rangle = E\{X|Y\}$, and from Lemma 3.4, we have

$$E \left\{ (X')^{Y+1} e^{-X'} | Y \right\} = \langle X \rangle e^{-\langle X \rangle} (Y + 1).$$

Substituting these into equation 41, we simplify to

$$I(X; Y_\delta) - I(X; Y) = \delta E\{X \log X - \langle X \rangle \log \langle X \rangle\} + o(\delta),$$

Dividing both sides by δ and taking the limit as $\delta \rightarrow 0$, we obtain

$$\left. \frac{d}{d\delta} I(X; Y_\delta) \right|_{\delta=0} = E[X \log X - \langle X \rangle \log \langle X \rangle],$$

where $\langle X \rangle = E[X|Y]$. This completes the proof of the lemma.

B. Tail Bounds

As we know the output z_γ given the input x is modeled as $z_\gamma \sim \mathcal{P}(\gamma x)$, where $x \geq 0$ is the non-negative input random variable, and γ represents the signal-to-noise ratio (SNR). The negative log-likelihood when estimating z_γ using x , is given by:

$$l(x, z_\gamma) = -\log p(z_\gamma|x) = -\log \left(\frac{e^{-\gamma x} (\gamma x)^{z_\gamma}}{z_\gamma!} \right) = \gamma x - z_\gamma \log(\gamma x) + \log z_\gamma!$$

We define the expected negative log-likelihood as $M(\gamma) = E_{(x, z_\gamma)} [l(x, z_\gamma)] = E_x [E_{z_\gamma|x} [l(x, z_\gamma)]]$. We now consider a mean constraint $\mu = E[x]$ in this case and our objective then is to determine the input distribution $p_X(x)$ over $x \geq 0$ that maximizes the above function. To compute the expected loss, let us first evaluate $E_{z_\gamma|x} [l(x, z_\gamma)]$ and using $E_{z_\gamma|x} [z_\gamma] = \gamma x$ gives:

$$E_{z_\gamma|x} [l(x, z_\gamma)] = E_{z_\gamma|x} [\gamma x - z_\gamma \log(\gamma x) + \log z_\gamma!] = \gamma x - \log(\gamma x) \cdot E_{z_\gamma|x} [z_\gamma] + E_{z_\gamma|x} [\log z_\gamma!] = \gamma x - \gamma x \log(\gamma x) + E_{z_\gamma|x} [\log z_\gamma!]$$

We can write $M(\gamma)$ in terms of the conditional entropy of z_γ given x as:

$$M(\gamma) = E_x [H(z_\gamma|x)], \text{ since } H(z_\gamma|x) = E_{z_\gamma|x} [-\log p(z_\gamma|x)] = E_{z_\gamma|x} [l(x, z_\gamma)].$$

The entropy $H(z_\gamma|x)$ of a Poisson distribution with parameter γx is given by:

$$HS(\gamma x) = -\sum_{k=0}^{\infty} P(z_\gamma = k) \log P(z_\gamma = k)$$

where $P(z_\gamma = k) = \frac{(\gamma x)^k e^{-\gamma x}}{k!}$. So substituting this into the entropy expression, we obtain:

$$HS(\gamma x) = -\sum_{k=0}^{\infty} \frac{(\gamma x)^k e^{-\gamma x}}{k!} \log \left(\frac{(\gamma x)^k e^{-\gamma x}}{k!} \right) = \gamma x - \gamma x \log(\gamma x) + \sum_{k=0}^{\infty} \frac{(\gamma x)^k e^{-\gamma x}}{k!} \log k!$$

It is natural to assume that the Shannon entropy $HS(\lambda)$ of a Poisson distribution strictly increases with $\lambda \in (0, +\infty)$. We will prove this result, as well as the concavity property of $HS(\lambda)$, in the following lemma.

Lemma B.1. *The Shannon entropy $HS(\lambda)$, $\lambda \in (0, +\infty)$, is strictly increasing and concave in λ .*

Proof. The Shannon entropy $HS(\lambda)$ of a Poisson distribution is as outlined above. To analyze the monotonicity and concavity of $HS(\lambda)$, we compute its first and second derivatives with respect to λ .

First, the first derivative $HS'(\lambda)$ is:

$$H'_S(\lambda) = -\log\left(\frac{\lambda}{e}\right) - 1 - e^{-\lambda} \sum_{k=2}^{\infty} \frac{\lambda^k \log k!}{k!} + e^{-\lambda} \sum_{k=2}^{\infty} \frac{\lambda^{k-1} \log k!}{(k-1)!} = -\log \lambda + e^{-\lambda} \sum_{k=1}^{\infty} \frac{\lambda^k \log(k+1)!}{k!} - e^{-\lambda} \sum_{k=2}^{\infty} \frac{\lambda^k \log k!}{k!}$$

Simplifying, we get:

$$HS'(\lambda) = -\log \lambda + e^{-\lambda} \sum_{k=1}^{\infty} \frac{\lambda^k}{k!} \log(k+1)$$

It is clear that both terms on the right-hand side of (2) are non-negative for $\lambda \in (0, 1]$, and the second term is strictly positive. Therefore, $H'_S(\lambda) > 0$ for $\lambda \in (0, 1]$. Now, it remains to prove that $H'_S(\lambda) > 0$ for $\lambda > 1$. Let's calculate:

$$\begin{aligned} H''_S(\lambda) &= -\frac{1}{\lambda} - e^{-\lambda} \sum_{k=1}^{\infty} \frac{\lambda^k \log(k+1)}{k!} + e^{-\lambda} \sum_{k=1}^{\infty} \frac{\lambda^{k-1} \log(k+1)}{(k-1)!} \\ &= -\frac{1}{\lambda} + e^{-\lambda} \sum_{k=0}^{\infty} \frac{\lambda^k \log(k+2)}{k!} - e^{-\lambda} \sum_{k=1}^{\infty} \frac{\lambda^k \log(k+1)}{k!} \\ &= -\frac{1}{\lambda} + e^{-\lambda} \log 2 + e^{-\lambda} \sum_{k=1}^{\infty} \frac{\lambda^k \log\left(1 + \frac{1}{k+1}\right)}{k!} \\ &= -\frac{1}{\lambda} + e^{-\lambda} \sum_{k=0}^{\infty} \frac{\lambda^k \log\left(1 + \frac{1}{k+1}\right)}{k!} \\ &< -\frac{1}{\lambda} + e^{-\lambda} \sum_{k=0}^{\infty} \frac{\lambda^k}{(k+1)!} < -\frac{1}{\lambda} + e^{-\lambda} \frac{1}{\lambda} \sum_{k=0}^{\infty} \frac{\lambda^{k+1}}{(k+1)!} \\ &< -\frac{1}{\lambda} + e^{-\lambda} \frac{1}{\lambda} e^{\lambda} = 0. \end{aligned}$$

So, $H''_S(\lambda) < 0$ for all $\lambda > 0$. Therefore, $H'_S(\lambda)$ strictly decreases in λ , proving **concavity** and it is sufficient to prove that $\lim_{\lambda \rightarrow \infty} H'_S(\lambda) \geq 0$. After further simplification,

$$\lim_{\lambda \rightarrow \infty} H'_S(\lambda) = \lim_{\lambda \rightarrow \infty} \log \lambda \left(e^{-\lambda} (\log \lambda)^{-1} \sum_{k=1}^{\infty} \frac{\lambda^k \log(k+1)}{k!} - 1 \right),$$

and it is sufficient to establish that

$$\liminf_{\lambda \rightarrow \infty} e^{-\lambda} (\log \lambda)^{-1} \sum_{k=1}^{\infty} \frac{\lambda^k \log(k+1)}{k!} \geq 1.$$

This inequality is outlined in (Braiman et al., 2024). Using this, we get that $H'_S(\lambda) > 0$ for all $\lambda \geq 0$ and $H''_S(\lambda) < 0$ for all $\lambda \geq 0$, hence the proof follows.

Given that $H(z_\gamma|x)$ is an increasing and concave function of x for $x > 0$, we aim to maximize $E_x[H(z_\gamma|x)]$ under the mean constraint $E[x] = \mu$. The functional to maximize is $J[p_X(x)] = \int_0^\infty H(z_\gamma|x) p_X(x) dx$, subject to the normalization and mean constraints: $\int_0^\infty p_X(x) dx = 1$ and $\int_0^\infty x p_X(x) dx = \mu$

Introducing Lagrange multipliers λ and ν for these constraints, the Lagrangian becomes:

$$\mathcal{L}[p_X(x)] = \int_0^\infty H(z_\gamma|x)p_X(x) dx - \lambda \left(\int_0^\infty p_X(x) dx - 1 \right) - \nu \left(\int_0^\infty xp_X(x) dx - \mu \right)$$

Taking the functional derivative of \mathcal{L} with respect to $p_X(x)$ and setting it to zero for optimality yields: $\frac{\delta \mathcal{L}}{\delta p_X(x)} = H(z_\gamma|x) - \lambda - \nu x = 0$

Given the properties of $H(z_\gamma|x)$, the solution corresponds to an exponential distribution. The exponential distribution with mean μ is given by:

$$p_X(x) = \frac{1}{\mu} e^{-x/\mu}, \quad x \geq 0$$

Maximizing the entropy of x leads to a distribution that spreads the probability mass, thereby increasing uncertainty and consequently maximizing the mmle. Now, using this exponential prior, we will derive an expression for $\text{mmle}(\gamma)$ which we use for deriving the left and right tail bounds.

Now, the prior distribution for X is assumed to be an exponential distribution:

$$f_X(x) = \lambda e^{-\lambda x}$$

We introduce the latent variable Z_γ such that:

$$P(Z_\gamma = z|X = x) = \frac{e^{-\gamma x} (\gamma x)^z}{z!}$$

which follows a Poisson distribution. The conditional density of X given $Z_\gamma = z$ is derived as:

$$\begin{aligned} f_{X|Z}(x|z) &= \frac{P(Z_\gamma = z|X = x)f_X(x)}{P(Z_\gamma = z)} \\ f_{X|Z}(x|z) &= \frac{(\beta x)^z}{z!} \lambda e^{-\lambda x} e^{-\beta x} \\ &= \frac{(\beta x)^z \lambda e^{-(\lambda+\beta)x}}{z! P(Z_\gamma = z)} \end{aligned}$$

and we can notice that this is a Gamma distribution: $X|Z_\gamma = z \sim \text{Gamma}(z+1, \lambda+\beta)$ The posterior mean of X given Z_γ is:

$$E[X|Z_\gamma = z] = \frac{z+1}{\lambda+\beta} \quad (42)$$

and this serves as the optimal estimate \hat{X}^* . Now, let us consider the following expectation: (where l is the previously defined Poisson loss function)

$$E_{X|Z_\gamma} [l(X, X^*)] = E[X \log \left(\frac{X}{X^*} \right) - X + X^*] = E \left[X \log \left(\frac{X}{X^*} \right) | Z_\gamma \right] - E[X|Z_\gamma] + X^* \quad (43)$$

Using integration by parts and properties of the Gamma function, if $W \sim \text{Gamma}(\alpha, \beta)$, then: (Miller, 2006)

$$E[W \log W] = \frac{\alpha}{\beta} [\psi(\alpha+1) - \log \beta]$$

where we defined the **digamma function** $\psi(\alpha)$ as: $\psi(\alpha) = \frac{d}{d\alpha} \log \Gamma(\alpha)$ The above results would also follow from differentiating the moment formula:

$$E[X^n] = \frac{\Gamma(\alpha+n)}{\Gamma(\alpha)\beta^n}$$

Applying this result in our case gives us:

$$E[X \log X | Z_\gamma] = \frac{z+1}{\lambda+\beta} [\psi(z+2) - \log(\lambda+\alpha)]$$

We also have from Equation. 42:

$$\log(X^*) = \log(z+1) - \log(\lambda+\alpha)$$

Taking expectation, the first term in 43 can be written as:

$$E \left[X \log \left(\frac{X}{X^*} \right) \middle| Z \right] = \frac{z+1}{\lambda+\beta} [\psi(z+2) - \log(\lambda+\alpha)] - \frac{z+1}{\lambda+\alpha} [\log(z+1) - \log(\lambda+\alpha)] = \frac{z+1}{\lambda+\beta} [\psi(z+2) - \log(z+1)] \quad (44)$$

Now, we compute the marginal distribution as follows:

$$P(Z_\gamma = z) = \int_0^\infty P(Z_\gamma = z | X = x) f_X(x) dx = \frac{\lambda\beta^z}{z!} \int_0^\infty x^z e^{-(\lambda+\beta)x} dx.$$

Using the Gamma integral property stated as follows:

$$\int_0^\infty x^z e^{-(\lambda+\beta)x} dx = \frac{\Gamma(z+1)}{(\lambda+\beta)^{z+1}},$$

we obtain (since $\Gamma(z+1) = z!$):

$$P(Z_\gamma = z) = \frac{\lambda\beta^z}{z!} \cdot \frac{\Gamma(z+1)}{(\lambda+\beta)^{z+1}} = \frac{\lambda\beta^z}{(\lambda+\beta)^{z+1}} = (1-p)p^z, \text{ where } p = \frac{\beta}{\lambda+\beta}$$

Now, the $\text{mmle}(\gamma)$ expression obtained is as follows:

$$\text{mmle}(\gamma) = \sum_{z=0}^{\infty} (1-p)p^z \left[\frac{z+1}{\lambda+\beta} [\psi(z+2) - \log(z+1)] \right] = \frac{\lambda}{(\lambda+\beta)^2} \sum_{z=0}^{\infty} (z+1)p^z [\psi(z+2) - \log(z+1)].$$

B.1. Left Tail Bound

In case of (γ_0, γ_1) being the relevant range of integration, the left tail integral is defined as: $\int_0^{\gamma_0} \text{mmle}(\gamma) d\gamma$

First, we interchange the sum and the integral:

$$\int_0^{\gamma_0} \text{mmle}(\gamma) d\gamma = \sum_{z=0}^{\infty} (z+1) [\psi(z+2) - \log(z+1)] \int_0^{\gamma_0} \frac{\lambda}{(\lambda+\gamma)^2} \left(\frac{\gamma}{\lambda+\gamma} \right)^z d\gamma.$$

We define the inner integral as

$$I_z = \int_0^{\gamma_0} \frac{\lambda}{(\lambda+\gamma)^2} \left(\frac{\gamma}{\lambda+\gamma} \right)^z d\gamma.$$

Substitute $u = \lambda + \gamma$, which implies $\gamma = u - \lambda$ and $d\gamma = du$. The bounds change accordingly: $u = \lambda$ when $\gamma = 0$ and $u = \lambda + \gamma_0$ when $\gamma = \gamma_0$. The integral becomes

$$I_z = \lambda \int_{\lambda}^{\lambda+\gamma_0} \frac{(u-\lambda)^z}{u^{z+2}} du.$$

Next, using the substitution $v = \frac{u-\lambda}{u}$, leading to $u = \frac{\lambda}{1-v}$ and $du = \frac{\lambda}{(1-v)^2} dv$. The bounds transform to $v = 0$ when $u = \lambda$ and $v = \frac{\gamma_0}{\lambda+\gamma_0}$ when $u = \lambda + \gamma_0$. Substituting these into the integral yields

$$I_z = \int_0^{\frac{\gamma_0}{\lambda+\gamma_0}} v^z dv.$$

The integral I_z can be evaluated as

$$I_z = \left[\frac{v^{z+1}}{z+1} \right]_0^{\frac{\gamma_0}{\lambda+\gamma_0}} = \frac{\left(\frac{\gamma_0}{\lambda+\gamma_0} \right)^{z+1}}{z+1}.$$

Substituting I_z back into the expression for the expectation, gives:

$$\int_0^{\gamma_0} \text{mmle}(\gamma) d\gamma = \sum_{z=0}^{\infty} [\psi(z+2) - \log(z+1)] \left(\frac{\gamma_0}{\lambda+\gamma_0} \right)^{z+1}$$

Let the above sum be S which we use in the sections below. By re-indexing the sum with $k = z + 1$, the final result can more elegantly be expressed as:

$$\int_0^{\gamma_0} \text{mmle}(\gamma) d\gamma = \sum_{k=1}^{\infty} [\psi(k+1) - \log(k)] \left(\frac{\gamma_0}{\lambda+\gamma_0} \right)^k.$$

We aim to establish an upper bound for the sum

$$S = \sum_{z=0}^{\infty} (z+1) [\psi(z+2) - \log(z+1)] \left(\frac{\gamma_0}{\lambda+\gamma_0} \right)^{z+1},$$

where ψ denotes the digamma function, $\gamma_0 > 0$, and $\lambda > 0$.

Let us define $x = \frac{\gamma_0}{\lambda+\gamma_0}$. Given that $\gamma_0 > 0$ and $\lambda > 0$, it follows that $0 < x < 1$. From, (Abramowitz & Stegun, 1964), we recall the expansion of the digamma function:

$$\psi(z+2) = H_{z+1} - \gamma_E,$$

where H_n is the n -th harmonic number and γ_E is the Euler-Mascheroni constant. For large z ,

$$H_{z+1} = \log(z+1) + \gamma_E + \frac{1}{2(z+1)} - \frac{1}{12(z+1)^2} + \dots.$$

Substituting this into the expression for $\psi(z+2)$ yields:

$$\psi(z+2) - \log(z+1) = \frac{1}{2(z+1)} - \frac{1}{12(z+1)^2} + \dots.$$

From this expansion, it is evident that

$$\psi(z+2) - \log(z+1) < \frac{1}{2(z+1)}$$

for all $z \geq 0$, since the higher-order terms $-\frac{1}{12(z+1)^2} + \dots$ contribute negatively, thereby decreasing the overall value.

Consequently, each term in the sum satisfies

$$(z+1) [\psi(z+2) - \log(z+1)] x^{z+1} < \frac{1}{2} x^{z+1}.$$

Summing over z from 0 to ∞ , we obtain

$$S < \frac{1}{2} \sum_{z=0}^{\infty} x^{z+1}.$$

Using the simplification of the geometric series $\sum_{z=0}^{\infty} x^{z+1}$

$$\sum_{z=0}^{\infty} x^{z+1} = \frac{x}{1-x} \implies S < \frac{1}{2} \frac{x}{1-x}.$$

Substituting back $x = \frac{\gamma_0}{\lambda + \gamma_0}$, we have

$$1 - x = 1 - \frac{\gamma_0}{\lambda + \gamma_0} = \frac{\lambda}{\lambda + \gamma_0} \implies \frac{x}{1 - x} = \frac{\frac{\gamma_0}{\lambda + \gamma_0}}{\frac{\lambda}{\lambda + \gamma_0}} = \frac{\gamma_0}{\lambda}.$$

Putting this into the inequality for S , we obtain

$$S < \frac{1}{2} \frac{\gamma_0}{\lambda}.$$

Hence, the upper bound for the sum in the scalar case (for a single input-output realization) is

$$\sum_{z=0}^{\infty} (z+1) [\psi(z+2) - \log(z+1)] \left(\frac{\gamma_0}{\lambda + \gamma_0} \right)^{z+1} \leq \frac{\gamma_0}{2\lambda}.$$

(**Note:** This z is different from the z_γ notation used throughout the paper.)

Extending this result to the vector case, consider a d -dimensional random vector $x \in X \subset \mathbb{Z}^d$ with covariance matrix Σ , whose eigenvalues are $\{\lambda_i\}_{i=1}^d$, all positive. Assuming the problem is separable across the eigenbasis of Σ , each dimension can be treated independently.

For the vector case, the sum becomes

$$S_{\text{vector}} = \sum_{i=1}^d \sum_{z=0}^{\infty} (z+1) [\psi(z+2) - \log(z+1)] \left(\frac{\gamma_0}{\lambda_i + \gamma_0} \right)^{z+1}.$$

Applying the scalar bound to each eigenvalue λ_i , we have

$$\sum_{z=0}^{\infty} (z+1) [\psi(z+2) - \log(z+1)] \left(\frac{\gamma_0}{\lambda_i + \gamma_0} \right)^{z+1} \leq \frac{\gamma_0}{2\lambda_i}.$$

Summing over all i from 1 to d , the vector sum satisfies

$$S_{\text{vector}} \leq \sum_{i=1}^d \frac{\gamma_0}{2\lambda_i} = \frac{\gamma_0}{2} \sum_{i=1}^d \frac{1}{\lambda_i}.$$

In the special case where the covariance matrix Σ is isotropic, meaning all eigenvalues $\lambda_i = \lambda$ for $i = 1, \dots, d$, the bound simplifies to

$$S_{\text{vector}} \leq \frac{d\gamma_0}{2\lambda}.$$

This concludes the derivation of the left tail bounds for both the scalar and vector cases.

B.2. Right Tail Bound

In case of (γ_0, γ_1) being the relevant range of integration, the right tail integral is defined as: $\int_{\gamma_1}^{\infty} \text{mmle}(\gamma) d\gamma$

Consider a discrete variable $x = (x_1, x_2, \dots, x_d) \in X \subset \mathbb{Z}^d$, where each component x_i belongs to a discrete set $\{i \Delta \mid i \in \mathbb{Z}\}$. Observations are modeled as $z_{\gamma,i} \sim \mathcal{P}(\gamma x_i)$ for a large signal-to-noise ratio (SNR) parameter γ . The estimator $\hat{x}_i(z_{\gamma,i})$ is typically the maximum likelihood estimator (MLE), implemented by rounding $z_{\gamma,i}$ to the nearest bin $\{k \Delta\}$.

The loss function per component is defined as

$$L(x_i, \hat{x}_i) = x_i \log \left(\frac{x_i}{\hat{x}_i} \right) - x_i + \hat{x}_i,$$

and the $\text{mmle}(\gamma)$ is given by $\mathbb{E}[L(x_i, \hat{x}_i)]$ over the randomness of $z_{\gamma,i}$. The right-tail integral of interest is

$$I_R = \int_{\gamma_1}^{\infty} E \left[\sum_{i=1}^d L(x_i, \hat{x}_i(z_{\gamma,i})) \right] d\gamma,$$

which we aim to upper bound.

At high SNR ($\gamma \rightarrow \infty$), the noise is relatively small compared to x_i , but rare rounding errors of size $j\Delta$ can still occur. Focusing on a single component x_i , an error of size $j\Delta$ happens if

$$\hat{x}_i = x_i - j\Delta \iff z_{\gamma,i} \in [\gamma(x_i - j\Delta - 0.5\Delta), \gamma(x_i - j\Delta + 0.5\Delta)).$$

For $z_{\gamma,i} \sim \text{Poisson}(\mu)$ with $\mu = \gamma x_i$, the Poisson Chernoff bound (Chernoff, 1952) provides that the probability of such a deviation is at most $\exp(-c_{i,j}\gamma)$, where $c_{i,j} > 0$ is a constant dependent on Δ , x_i , and the shift $j\Delta$. Hence,

$$P(\text{error of size } j\Delta) \leq e^{-c_{i,j}\gamma}.$$

The per-component contribution to the mean MLE loss is

$$\text{mmle}_i(\gamma) = E_{z_{\gamma,i}} [L(x_i, \hat{x}_i(z_{\gamma,i}))].$$

When the estimation error is $j\Delta$, the loss becomes

$$L(x_i, x_i - j\Delta) = x_i \log \left(\frac{x_i}{x_i - j\Delta} \right) - x_i + (x_i - j\Delta).$$

Therefore, the mean loss satisfies

$$\text{mmle}_i(\gamma) \leq \sum_{j=1}^{j_{\max}} \left[x_i \log \left(\frac{x_i}{x_i - j\Delta} \right) - x_i + (x_i - j\Delta) \right] e^{-c_{i,j}\gamma}.$$

Summing over all components $i = 1, \dots, d$, we obtain

$$\text{mmle}(\gamma) = \sum_{i=1}^d \text{mmle}_i(\gamma) \leq \sum_{i=1}^d \sum_{j=1}^{j_{\max}} \left[x_i \log \left(\frac{x_i}{x_i - j\Delta} \right) - x_i + (x_i - j\Delta) \right] e^{-c_{i,j}\gamma}.$$

The right-tail integral I_R can thus be bounded as

$$I_R = \int_{\gamma_1}^{\infty} \text{mmle}(\gamma) d\gamma \leq \sum_{i=1}^d \sum_{j=1}^{j_{\max}} \left[x_i \log \left(\frac{x_i}{x_i - j\Delta} \right) - x_i + (x_i - j\Delta) \right] \int_{\gamma_1}^{\infty} e^{-c_{i,j}\gamma} d\gamma.$$

Evaluating the integral, we find

$$\int_{\gamma_1}^{\infty} e^{-c_{i,j}\gamma} d\gamma = \frac{e^{-c_{i,j}\gamma_1}}{c_{i,j}},$$

Leading to the final right-tail bound

$$I_R = \int_{\gamma_1}^{\infty} E \left[\sum_{i=1}^d L(x_i, \hat{x}_i) \right] d\gamma \leq \sum_{i=1}^d \sum_{j=1}^{j_{\max}} \left[x_i \log \left(\frac{x_i}{x_i - j\Delta} \right) - j\Delta \right] \frac{e^{-c_{i,j}\gamma_1}}{c_{i,j}}.$$

In the above expression, $c_{i,j} > 0$ represents the Chernoff-type exponent from the Poisson large-deviation bound for the event causing an error of size $j\Delta$ in component i . We determine these parameters empirically, and the parameter j_{\max} indicates the largest error shift considered, which is typically small in practice and can be tuned empirically.

For empirical purposes, it might also be worthwhile to note that the bracketed term in 44 can be approximated as the sum over a few starting z beyond which it effectively dies out:

C. Proof of Pointwise Poisson Denoising Relation

For Poisson channel observations $Z_\gamma \sim \text{Poisson}(\gamma X)$, we derive the pointwise denoising relation:

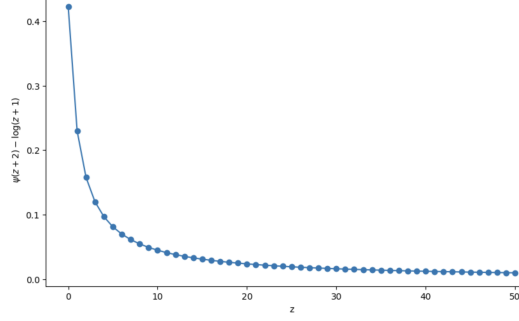


Figure 8. Approximating the Digamma term

Theorem C.1. *The KL divergence derivative satisfies:*

$$\frac{d}{d\gamma} D_{KL}[P(z_\gamma|x) \| P(z_\gamma)] = \text{mmle}(x, \gamma)$$

where the pointwise MMLE is:

$$\text{mmle}(x, \gamma) \equiv E_{P(z_\gamma|x)} [l(x, \hat{x}^*(z_\gamma))]$$

with $l(x, x^*) = x \log \frac{x}{x^*} - x + x^*$ and $\hat{x}^*(z_\gamma) = E[X|z_\gamma]$.

Proof: By definition,

$$D_{KL}(P(Z_\gamma|X) \| P(Z_\gamma)) = E_{P(x)} [E_{P(z_\gamma|x)} [\log P(z_\gamma|x) - \log P(z_\gamma)]] .$$

We first move the differentiation inside expectations,

$$\frac{d}{d\gamma} D_{KL} = E_{P(x)} [E_{P(z_\gamma|x)} [\frac{d}{d\gamma} \log P(z_\gamma|x)]] - E_{P(x)} [E_{P(z_\gamma|x)} [\frac{d}{d\gamma} \log P(z_\gamma)]] .$$

For the Poisson distribution with mean γx ,

$$P(z_\gamma|x) = e^{-\gamma x} \frac{(\gamma x)^{z_\gamma}}{z_\gamma!} .$$

Taking the derivative,

$$\frac{d}{d\gamma} \log P(z_\gamma|x) = -x + \frac{z_\gamma}{\gamma} .$$

Taking expectation w.r.t. $P(z_\gamma|x)$, the first term comes out to be zero.

$$E_{P(z_\gamma|x)} [-x + \frac{z_\gamma}{\gamma}] = -x + \frac{1}{\gamma} E_{P(z_\gamma|x)} [z_\gamma] = -x + \frac{\gamma x}{\gamma} = 0 .$$

For the marginal,

$$P(z_\gamma) = \int P(z_\gamma|x) P(x) dx .$$

Taking the log-derivative,

$$\frac{d}{d\gamma} \log P(z_\gamma) = \frac{1}{P(z_\gamma)} \int (-x + \frac{z_\gamma}{\gamma}) P(z_\gamma|x) P(x) dx .$$

Identifying this as a conditional expectation,

$$\frac{d}{d\gamma} \log P(z_\gamma) = E[-X + \frac{z_\gamma}{\gamma} | z_\gamma] .$$

Thus, the second term is

$$E_{P(x)}[E_{P(z_\gamma|x)}[\frac{d}{d\gamma} \log P(z_\gamma)]] = E_{P(z_\gamma|x)}[E[-X + \frac{z_\gamma}{\gamma} | z_\gamma]].$$

Combining both terms,

$$\begin{aligned} \frac{d}{d\gamma} D_{KL} &= 0 - E_{P(z_\gamma|x)}[E[-X + \frac{z_\gamma}{\gamma} | z_\gamma]]. \\ \frac{d}{d\gamma} D_{KL}(P(Z_\gamma|X) \| P(Z_\gamma)) &= E_{P(z_\gamma|x)}[E[X | z_\gamma] - \frac{z_\gamma}{\gamma}]. \end{aligned}$$

Link to the MMLE Loss. We already defined the loss function:

$$\ell(x, \hat{x}^*) = x \log \frac{x}{\hat{x}^*} - x + \hat{x}^*.$$

If $\hat{x}^* \equiv E[X | z_\gamma]$ is the estimator of x given z_γ , then by standard properties of conditional expectation,

$$E_{P(z_\gamma|x)}[\hat{x}^*] = E[E[X | z_\gamma]] = E[X] = x \quad (\text{if } x \text{ is deterministic, replace } E[X] \text{ by } x).$$

Hence,

$$E_{P(z_\gamma|x)}[\ell(x, \hat{x}^*)] = E[x \log x - x \log \hat{x}^* - x + \hat{x}^*] = x \log x - x - x E[\log \hat{x}^*] + E[\hat{x}^*].$$

Since $E[\hat{x}^*] = x$,

$$E_{P(z_\gamma|x)}[\ell(x, \hat{x}^*)] = x(\log x - E[\log \hat{x}^*]).$$

One can show (by comparing with the final expression in the KL derivative) that this expectation aligns with $E_{P(z_\gamma|x)}[E[X | z_\gamma] - \frac{z_\gamma}{\gamma}]$, thus establishing the link between the MMLE and the derivative of the KL divergence. We can generalize this relation to any loss function that belongs to the class of Bregman divergences in a Poisson channel using the framework described in (Wang et al., 2013).

C.1. Tweedie's for Poisson Denoising

A well-known result in Gaussian denoising is *Tweedie's Formula*, which expresses the conditional expectation of the latent variable in terms of the derivative of the log-pdf of noisy observation. (Robbins, 1956). Specifically, for $Z_\gamma = \sqrt{\gamma}X + \varepsilon$ with $\varepsilon \sim \mathcal{N}(0, I)$, we have:

$$E[X | Z_\gamma = z] = \frac{z}{\sqrt{\gamma}} + \frac{1}{\gamma} \nabla \log f_{Z_\gamma}(z), \quad (45)$$

In the Poisson setting, we cannot directly take derivatives of $\log P_{Z_\gamma}(z)$ with respect to discrete z since they are undefined. Instead, the *forward difference* of the log of the marginal PMF serves as a discrete analog. This culminates in the Turing-Good-Robbins (TGR) formula, already presented in Lemma 3.4:

Hence, just like Tweedie's Formula in the continuous Gaussian case, TGR expresses the conditional mean $\langle X \rangle_z$ purely in terms of the marginal distribution $P_{Z_\gamma}(z)$, bypassing any need to compute the conditional distribution $P_{X|Z_\gamma}$. In effect, the ratio $\gamma \cdot \langle X \rangle_z$ plays the role of a *score function* for the Poisson channel, analogous to the logarithmic derivative in the Gaussian case. This discrete variant underpins our Poisson diffusion framework, allowing us to efficiently compute the optimal denoiser $E[X | Z_\gamma]$ directly from the marginal PMF.

D. Continuous-Time Extension of ItDPDM

We extend the discrete-time channel with continuous states (DTCS) to continuous time through the following construction:

Definition D.1 (Continuous-Time Channel with States (CTCS)). Let $\{X_t\}_{t \geq 0}$ be a right-continuous state process with left limits (càdlàg) taking values in \mathbb{R}_+ . The output process $\{Y_t\}_{t \geq 0}$ is a counting process satisfying:

$$Y_t = \mathcal{P} \left(\int_0^t X_s ds \right) \quad (46)$$

where $\mathcal{P}(\cdot)$ denotes a Poisson counting measure.

For measurable intensity X_t , the output increments also satisfy:

$$Y_{t+\delta} - Y_t \sim \mathcal{P} \left(\int_t^{t+\delta} X_s ds \right), \quad \forall t, \delta \geq 0 \quad (47)$$

with $\{Y_{t_k} - Y_{t_{k-1}}\}_{k=1}^n$ independent given $X_{[0,T]}$ for any finite partition $\{t_k\}$.

The mutual information between state and observation processes over $[0, T]$ is given by:

$$I(X^T; Y^T) = E \left[\log \frac{dP_{Y^T|X^T}}{dP_{Y^T}} \right] \quad (48)$$

The key connection to discrete-time systems emerges through infinitesimal discretization:

Theorem D.2 (Mutual Information Rate). *For the CTCS in Definition D.1, the mutual information rate satisfies:*

$$\lim_{T \rightarrow \infty} \frac{1}{T} I(X^T; Y^T) = \lim_{\delta \rightarrow 0} \frac{1}{\delta} I(X_\delta; Y_\delta) \quad (49)$$

where $X_\delta := X_{[0,\delta]}$ and $Y_\delta := Y_\delta - Y_0$ corresponds to the discrete-time channel $\mathcal{P}(\delta X)$.

Proof Sketch. Consider time partitions $0 = t_0 < t_1 < \dots < t_n = T$ with $\max |t_{k+1} - t_k| \leq \delta$. By the chain rule of mutual information:

$$\begin{aligned} I(X^T; Y^T) &= \sum_{k=0}^{n-1} I(X^{t_{k+1}}; Y_{t_{k+1}} | Y^{t_k}) \\ &= \sum_{k=0}^{n-1} [I(X_{[t_k, t_{k+1}]}; Y_{[t_k, t_{k+1}]}) + \epsilon_k] \end{aligned}$$

where ϵ_k captures residual dependence between time intervals. Using the Markov property of Poisson counters (Davis, 1993) and taking $\delta \rightarrow 0$, the residual terms vanish by the Asymptotic Equipartition Property (AEP) for Poisson processes (Duncan, 1970). The result follows from Theorem A.3 applied to each infinitesimal interval.

The continuous-time counterpart of the derivative relationship becomes:

Theorem D.3 (Information Rate Derivative). *For the CTCS system, the time derivative of mutual information satisfies:*

$$\frac{d}{dt} I(X^t; Y^t) = E [X_t \log X_t - \langle X_t \rangle \log \langle X_t \rangle] \quad (50)$$

where $\langle X_t \rangle := E[X_t | Y^t]$ is the causal MMLE estimator.

Proof. From Theorem D.2 and the DTCS derivative, we have:

$$\begin{aligned} \frac{d}{dt} I(X^t; Y^t) &= \lim_{\delta \rightarrow 0} \frac{1}{\delta} [I(X_{t+\delta}; Y_{t+\delta} | Y^t) - I(X_t; Y_t)] \\ &= \lim_{\delta \rightarrow 0} \frac{1}{\delta} E [\delta X_t \log X_t - \delta \langle X_t \rangle \log \langle X_t \rangle] + o(1) \end{aligned}$$

The result follows by dominated convergence and the tower property of conditional expectation. This continuous-time formulation preserves the essential duality between information and estimation seen in discrete time, with the Poisson channel's inherent noise characteristics governing both regimes. The CTCS framework enables analysis of real-time filtering and prediction (Snyder, 1972) through differential versions of the key discrete-time identities.

E. Training Details

For a fair comparison, we train both CIFAR and LMD models from scratch for 50 epochs. The training starts with a learning rate of 2×10^{-5} using the Adam optimizer. We adopt an 80-20 train-test split for evaluating likelihoods. For image generation, we use a UNet-based model, while for music generation, we employ an NCSN-based model. The training procedure ensures consistency across both domains, facilitating a meaningful comparison of their performance.

E.1. Symbolic Music Dataset Preprocessing

We utilize the cleaned Lakh MIDI dataset (Vogl et al., 2017), loading note sequences from *.npy* files with original shape $(x, 1024)$. For training, sequences are partitioned into individual 1D vectors of shape $(1, 1024)$, representing discrete musical events. So, our method directly models symbolic music as discrete 1D note sequences using a Poisson-based diffusion process, avoiding hybrid architectures or preprocessing.

F. Noised and Denoised Image Comparison

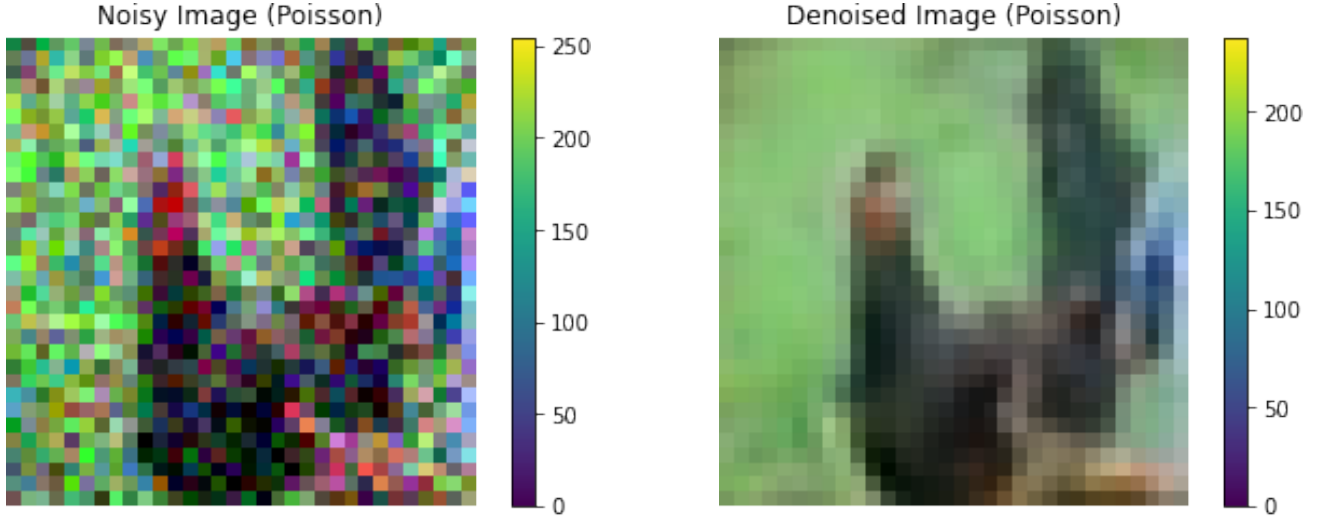


Figure 9. Noisy Image (Poisson Noise)
Noisy Image (Gaussian)

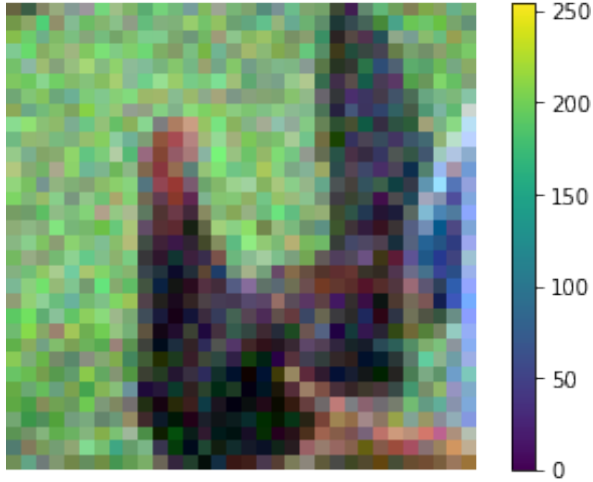


Figure 11. Noisy Image (Gaussian Noise)

Figure 10. Denoised Image (Poisson Noise)
Denoised Image (Gaussian)

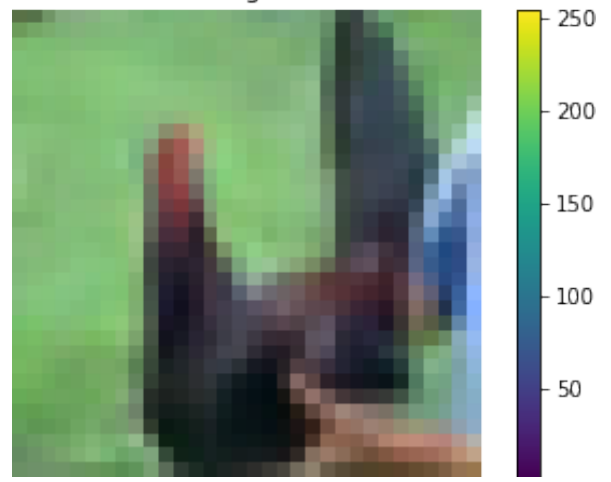


Figure 12. Denoised Image (Gaussian Noise)

Figure 13. Comparison of noisy and denoised images for poisoned and Gaussian noise birds with $\log\text{snr}=4.01$.

Figure 13 presents a comparison of noisy and denoised images under Gaussian and Poisson noise conditions at a $\log\text{SNR}$ of 4.01. The left column displays the input images corrupted by Gaussian (Figure 11) and Poisson noise (Figure 9), while the right column shows the corresponding denoised outputs (Figures 10 and Figures 10). Notably, the Poisson noise case exhibits a higher level of degradation than the Gaussian noise case, making recovery more challenging. However, the denoising process effectively reconstructs meaningful image structures in both cases, demonstrating the model's robustness to varying noise distributions.

G. Training and Sampling Pseudocode

Algorithm 1 ItDPDM Sampling

Trained model f_θ
 Number of reverse steps T
 Range of SNR (e.g. γ_{\max} down to γ_{\min})
 Find γ values corresponding to $t = T, \dots, 1$
 Initialize $\hat{z}_{\gamma_{\min}} \leftarrow 0$ (or minimal intensities)
 $t = T, \dots, 1$ Choose intermediate γ_t (e.g. spaced in log-SNR).
 Use denoiser: $\hat{x}_t = f_\theta(\text{data-transform}(\hat{z}_{\gamma_t}), \gamma_t)$
 Sample new $\hat{z}_{\gamma_{t-1}} \sim \text{Poisson}(\gamma_{t-1} \hat{x}_t)$
 Return final $\hat{x}_0 = (\hat{z}_{\gamma_0})$

(a) Sampling Pseudocode

Algorithm 1 ItDPDM Training

Dataset $\{x_i\}_{i=1}^N$ of nonnegative discrete samples
 Number of log-SNR samples S
 SNR range $[\gamma_{\min}, \gamma_{\max}]$
 Neural network $f_\theta(\cdot)$ for denoiser. Learned parameters θ .
 mini-batch B in dataset $s = 1$ to S
 Sample $\alpha \sim q(\alpha)$ (logistic distribution)
 Let $\gamma = \exp(\alpha)$
 Draw $z_\gamma \sim \text{Poisson}(\frac{\gamma x_B}{1+\gamma})$
 $\hat{x}_B = f_\theta(\text{data-transform}(z_\gamma), \gamma)$
 $\ell = \sum_{i \in B} \text{mle}(x_i, \hat{x}_i)$
 $L = \ell \times \frac{1}{q(\alpha)}$
 Gradient descent on L to update θ
 Return θ

(b) Training Pseudocode

Figure 14. Illustration of the sampling and training pseudocode used in our method.

H. Theoretical Runtime Analysis of ItDPDM Architecture

We present a theoretical runtime analysis of the proposed *Information-Theoretic Discrete Poisson Diffusion Model* (ItDPDM), focusing on the core components contributing to its computational cost during training and inference.

H.1. Poisson Noise Sampling

The forward diffusion process in ItDPDM is governed by a Poisson noise channel $z_\gamma \sim \text{Poisson}(\gamma x)$, where $x \in \mathbb{R}_+^D$ denotes the input data vector and γ is the signal-to-noise ratio (SNR). Sampling from a Poisson distribution can be performed in $\mathcal{O}(1)$ per element using rejection sampling or table-based methods, resulting in a total cost of $\mathcal{O}(D)$ per data point.

H.2. Neural Denoising

The denoiser is instantiated as a neural network, such as a U-Net (for images) or a Transformer encoder (for symbolic music). The input to the denoiser is the reparameterized form

$$\tilde{z}_\gamma = \frac{z_\gamma}{1 + \gamma},$$

which improves numerical stability. The forward pass of the denoiser has cost $\mathcal{O}(D)$ per data point, assuming conventional convolutional or attention-based layers.

H.3. Poisson Loss Function Evaluation

The proposed loss function is based on a Bregman divergence tailored to Poisson noise:

$$\ell(x, \hat{x}) = x \log \left(\frac{x}{\hat{x}} \right) - x + \hat{x},$$

which is convex, differentiable, and evaluated pointwise. The cost of loss evaluation and gradient computation is $\mathcal{O}(D)$ per sample.

H.4. Integral Estimation over SNR

A defining component of the ItDPDM framework is the estimation of the negative log-likelihood using thermodynamic integration:

$$-\log P(x) = \int_0^\infty \text{mmle}(x, \gamma) d\gamma,$$

where MMLE denotes the minimum mean likelihood error. In practice, this integral is approximated numerically using n log-SNR values (e.g., $n = 1000$), obtained via uniform or importance sampling over $\alpha = \log \gamma$.

Each SNR point requires a forward pass through the denoiser and loss computation, yielding a total per-sample complexity of $\mathcal{O}(n \cdot D)$. To reduce overhead, the model uses importance sampling from a truncated logistic distribution over α and closed-form tail integral bounds to truncate the SNR domain (see Eqs. (28)–(29) in the main text).

Component	Complexity	Description
Poisson noise sampling	$\mathcal{O}(D)$	Efficient per-sample noise generation
Neural denoising	$\mathcal{O}(D)$	Forward pass through CNN or Transformer
Poisson loss function	$\mathcal{O}(D)$	Evaluated pointwise for each data coordinate
Integral over SNR	$\mathcal{O}(n \cdot D)$	Dominant cost due to repeated inference and loss evaluations
Total per-sample cost	$\mathcal{O}(n \cdot D)$	For fixed number of SNR grid points

Table 3. Asymptotic complexity of key components in the ItDPDM training pipeline.

Given a batch size B and number of training epochs E , the overall training complexity becomes: $\mathcal{O}(B \cdot E \cdot n \cdot D)$. This is comparable to standard continuous-state diffusion models using discretized time steps, but the Poisson-specific formulation and MMLE integral introduce unique architectural and optimization challenges that are efficiently addressed via reparameterization and sampling strategies.